DEHLSEN
ASSOCIATES, LLC

Final Technical Report
DE-EE0007344
April 2016 - June 2020

Numerical Modeling and Experimental Validation of Extreme Conditions Response for the Centipod WEC

16 October 2020

Principle Investigator:
Alan McCall
amccall@ecomerittech.com
805-845-0496
Dehlsen Associates, LLC
101 E. Victoria Street, Suite F, Santa Barbara, CA 93101

U.S. Department of Energy Disclaimer

This report was prepared as an account of work partially sponsored by an agency of the United States Government. Neither the United States Government nor any agency thereof, nor any of their employees, makes any warranty, express or implied, or assumes any legal liability or responsibility for the accuracy, completeness, or usefulness of any information, apparatus, product, or process disclosed, or represents that its use would not infringe privately owned rights. Reference herein to any specific commercial product, process, or service by trade name, trademark, manufacturer, or otherwise does not necessarily constitute or imply its endorsement, recommendation, or favoring by the United States Government or any agency thereof. The views and opinions of authors expressed herein do not necessarily state or reflect those of the United States Government or any agency thereof.

Project Consortium Legal Notice/Disclaimer

This report was prepared by Dehlsen Associates, LLC pursuant to a Grant funded by the U.S. Department of Energy (DOE) under Instrument Number DE-EE0006404 NO WARRANTY OR REPRESENTATION, EXPRESS OR IMPLIED, IS MADE WITH RESPECT TO THE ACCURACY, COMPLETENESS, AND/OR USEFULNESS OF INFORMATION CONTAINED IN THIS REPORT. FURTHER, NO WARRANTY OR REPRESENTATION, EXPRESS OR IMPLIED, IS MADE THAT THE USE OF ANY INFORMATION, APPARATUS, METHOD, OR PROCESS DISCLOSED IN THIS REPORT WILL NOT INFRINGE UPON PRIVATELY OWNED RIGHTS. FINALLY, NO LIABILITY IS ASSUMED WITH RESPECT TO THE USE OF, OR FOR DAMAGES RESULTING FROM THE USE OF, ANY INFORMATION, APPARATUS, METHOD OR PROCESS DISCLOSED IN THIS REPORT.

NOTE:

For further information about Dehlsen Associates, LLC, call 805-845-7575 or e-mail Alan McCall at amccall@ecomerittech.com.

Copyright © 2020 Dehlsen Associates, LLC. All rights reserved.

This publication is a corporate document that should be cited in the literature in the following manner: "Numerical Modeling and Experimental Validation of Extreme Conditions Response for the Centipod WEC". Dehlsen Associates, LLC, Santa Barbara, CA and U.S. Department of Energy, Washington, DC. 2020.

This material is based upon work supported by the U.S. Department of Energy's Office of Energy Efficiency and Renewable Energy (EERE) under the Water Power Technologies Office award number DE-EE0007344.

Long-term development of the Centipod Wave Energy Converter including the accomplishments discussed herein would not have been possible without the support and vision of many DOE project managers.

Contents

Contractual Information

Federal Agency to which Report is submitted: DOE EERE – Wind & Water Power Program

Recipient: Dehlsen Associates, LLC - DUNS 830226317
Award Number: DE-EE0007344
Project Title: Numerical Modeling and Experimental Validation of Extreme Conditions Response for the Centipod WEC
Project Period: Apr 1, 2016 to Jun 30, 2020
Principle Investigator:
Alan McCall, amccall@ecomerittech.com; 101 E. Victoria Street, Suite F, Santa Barbara, CA 93101; 805-845-0496
Report Submitted by:
Dave Arthurs, CFO, darthurs@ecomerittech.com; 101 E. Victoria Street, Suite F, Santa Barbara, CA 93101; 805-845-9101

Date of Report: Oct 16, 2020
Covering Period: Apr 1, 2016 to Jun 30, 2020
Working Partners:
Yi-Hsiang Yu
National Renewable Energy Laboratory
yi-hsiang.yu@nrel.gov
303-387143

Ryan Coe
Sandia National Laboratories
ryan.coe@sandia.gov
505-845-9064

Jarett Goldsmith
DNV-GL
jarett.goldsmith@dnvgl.com
858-836-3370

Samantha Lee
Naval Surface Warfare Center Carderock Division
richard.banko@navy.mil
301-227-1811

DOE Project Team: DOE HQ Program Manager – Alejandro Moreno
DOE Field Contract Officer – Laura Merrick
DOE Field Project Officer – Corey Vezina
DOE Award Administrator – Laura Rios

1.0 Executive Summary

As is often said, in wave energy conversion you pay for the peaks and get paid for the averages [1]. While loads drive the structural design, large loads result in large, costly structures dominating the capital expense of a wave energy converter [2]. Already a challenge for normal operating conditions, this becomes a serious barrier to economic viability when designing for extreme conditions that stem from 100-year storms. Since the early days of wave energy conversion research, minimizing extreme condition loads has been a headline design objective. This project continues the line of research in a quest for survivable wave energy converters (WECs).

It has been well established that the most straightforward method of building a survivable wave energy converter is to simply avoid the hydrodynamic excitation force (Fe) associated with infrequent, but damaging, storm events. To decouple from excitation force, a primary attempt is often made to detune from the exciting wave frequency through the use of controls. However, this has limitations as it can only reduce extreme loads so much. Due to these limitations, the approach of partially or fully submerging the WEC is often considered as well. Submergence is a credible solution as it undoubtedly reduces excitation force. However, submergence inherently requires a voluntary shedding of reserve buoyancy, creating a failure mode that climbs to the top of failure modes tables. Nevertheless, submergence generally remains a popular design choice. This project adds another option to the table by exploring the implementation of an additional degree of freedom not for power extraction purposes, but instead for extreme load reduction.

WEC degrees of freedom are expensive. The majority of WECs currently in development choose to exploit only one degree of freedom (DOF) whether it be heave, pitch, or surge. While multi-DOF WECs do exist, these additional degrees of freedom were often incorporated in the conceptual stage of design for increased power capture. For this design option to be viable, the cost of an additional DOF implementation must be clearly outweighed by the cost of inaction, in this case higher baseline design loads. This project shows that the choice of a secondary DOF for survivability is indeed a viable option. In the example case-study using Dehlsen Associates' "Centipod" WEC, an 8% reduction in LCOE was calculated as the result of this load mitigation degree of freedom approach, exceeding the originally proposed percentage-based LCOE improvement metric in this project.

This report will cover the calculation of the concluded LCOE advantage, but will also discuss the entire project from start to finish, including mid and high-fidelity modelling, survival mode trade study, wave basin testing, and design tool cross-verification and validation.

2.0 Technology Background

The Centipod Wave Energy Converter (WEC) is comprised of multiple point-absorber buoys which heave with passing waves. These point-absorber buoys, called “Pods”, react against a submerged, stable, common platform called the “Backbone” allowing for power extraction through a power take-off system between the Pods and Backbone.

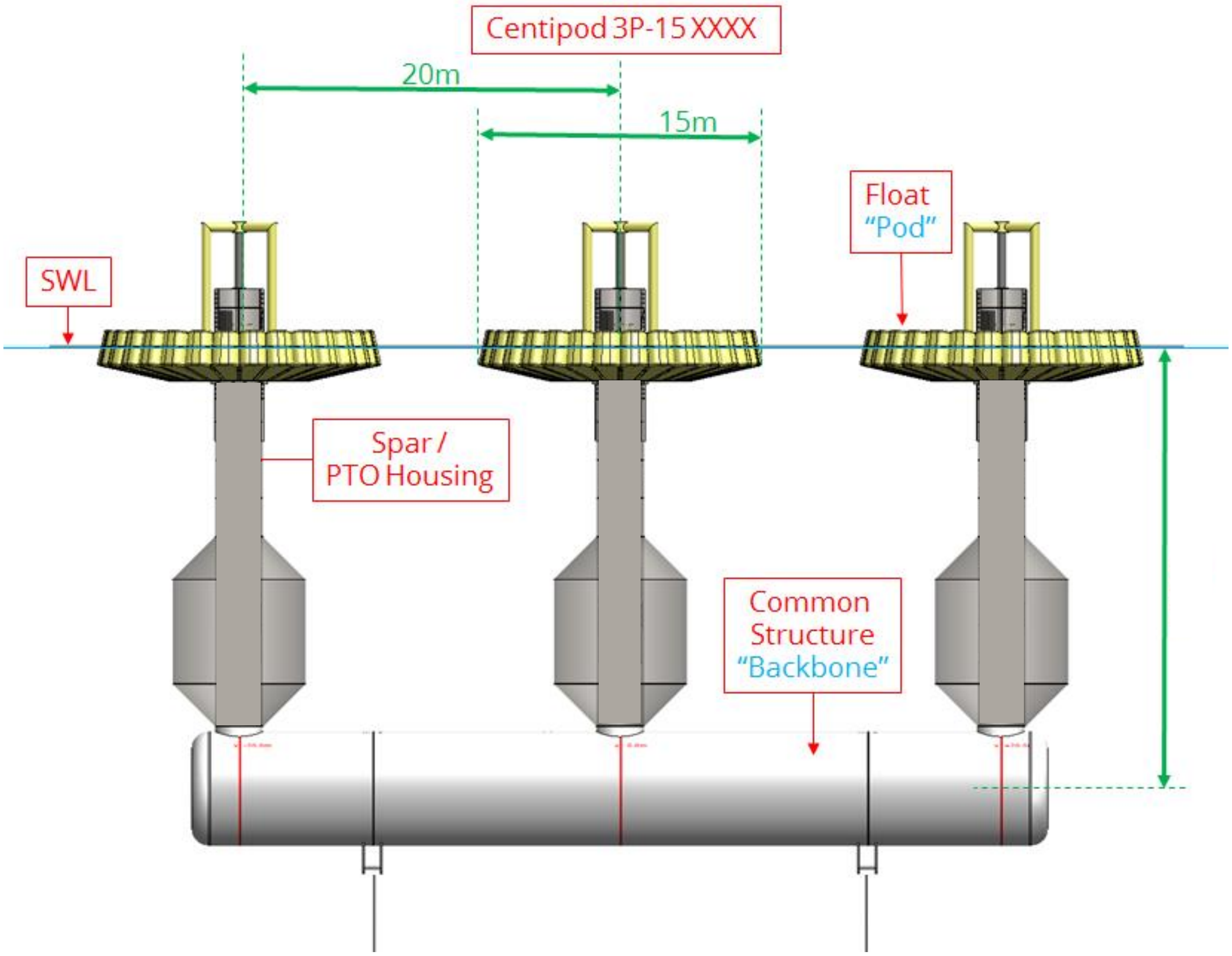

Figure 1 – General configuration and dimensiond of Centipod WEC

The specific design variant of the Centipod WEC used in this project consists of three 15-meter diameter axisymmetric Pods which have 1 degree of freedom in the heave direction. The Pods are connected, via a spar which also houses the power take-off unit, to a tension leg moored common Backbone that provides pre-tension to the mooring lines.

3.0 Proposed Project Parameters

3.1 Project Objectives

Dehlsen Associates, LLC (DA) planned to advance the design of Centipod for survivability while improving the understanding of mid and high-fidelity tools as they pertain to Extreme Condition Modeling (ECM). This work aimed to result in a more appropriate structural design of Centipod due to greater extreme conditions loads understanding and reduction of over designed structural components. The culmination of this project was also designed to result in a greater understanding of the accuracy and reliability of mid- and high-fidelity design tools (WaveDyn and computational fluid dynamics (CFD) respectively) for estimating extreme loads.

3.2 Project Scope

Dehlsen Associates developed a comprehensive work plan that aligned well with the technical objectives of the FOA[3]. The scope of work included Extreme Condition Modeling (ECM) using WaveDyn, CFD, and finite element analysis (FEA). Modeling of extreme conditions loads was to be validated via wave tank testing at the Navy's Carderock MASK (maneuvering and seakeeping basin) facility. The following is an overview of the tasks as originally planned at the beginning of the project.

3.3 Tasks Performed

3.3.1 - Task 1.0 Establish baseline design requirements

Establish design requirements for Centipod as they pertain to structural design and associated factors of safety. A design requirements document will be drafted which will establish the environmental conditions and design load cases (DLCs) relevant to this project, and the larger Centipod design.

3.3.2 - Task 2.0 Improved WEC design

A study of each DLC will be carried out in WaveDyn, followed by design revisions per the requirements set forth in Task 1. Using an existing mid-fidelity model of Centipod in WaveDyn, DA will analyze the extreme condition ultimate loads pertaining to each DLC defined in the baseline design requirements. This work will also lead to a down select of ultimate DLCs for experimental testing, based on those which appear most critical.

3.3.3 - Task 3.0 Design scale WEC model for test

Complete preliminary design of the scaled model. DA will design a scaled model of Centipod wave energy converter for wave tank testing. Scaling studies will be done to evaluate the best scale for testing. Numerical studies will be done on the scaled model using WAMIT and WaveDyn.

3.3.4 - Task 4.0 Build scale model for test

DA will work with NSWCCD (Naval Surface Warfare Center Carderock Division) to fabricate the scaled model of Centipod for testing. Any sensors required to be integrated into the model structure will be assembled. Prior to testing, each structural component's mass and geometry will be measured for future numerical model validation purposes to ensure effective model tuning.

3.3.5 - Task 5.0 Wave tank testing

DA is proposing to conduct a wave tank test at NSWCCD's Maneuvering and Seakeeping Basin (MASK) facility at Carderock, MD, a state-of-the-art deep-water wave basin with the ability to generate regular and irregular waves. DA will work with partners to plan, execute, and report on testing as described in the subtasks below.

3.3.6 - Task 6.0 Mid fidelity modeling of WEC at scale

Complete analysis in WaveDyn to match tank-tested parameters. DA will work with partners to build, run, and tune a WaveDyn model reflecting the wave basin testing to validate the mid-fidelity modeling.

3.3.7 - Task 7.0 High fidelity modeling of WEC at scale

DA, with NREL, will perform additional simulations in high and extreme sea states. The cases of most interest for high-fidelity analysis will likely be non-linear hydrodynamic events such as wave breaking and slamming. Wave basin testing and multi-body calculations performed in WaveDyn will allow for selection of a subset of Ultimate DLCs to be focused on for high fidelity modeling. Best practices and lessons learned from NREL's previous studies will be used in this analysis to ensure sound methodology.

3.3.8 - Task 8.0 Impact analysis

Analysis will be carried out on the impacts of the newly defined loads resulting from extreme conditions as it relates to the metrics set in the application. The experimental data, as well as the model predictions, will be used to analyze the impact of this study on our understanding of each tool's validity. The completion of this task will also lead to redefined design requirements.

3.3.9 - Task 9.0 MHK Risk and Reliability

The project risk management plan will be developed and address all aspects and methodologies DA will use to control project risks. DA will use DOE's MHK Risk Management Framework to identify and mitigate risks for this project. DA and its partners have identified the key risks associated with executing the proposed project. A key element of the risk management plan is the risk register, which can be used to document the risks and their severity level. The risk management plan will be periodically revisited to identify any new risks and track the existing ones.

4.0 Project Organization

Dehlsen Associates took on this project with the support of working partners with expertise in both physical model testing and numerical modeling of Wave Energy Converters. The National Renewable Energy Laboratory (NREL) and Sandia National Laboratories were the leading working partners in the domain of high-fidelity modelling and were joined by DNV-GL in the mid-fidelity modelling expertise area. Meanwhile, Naval Surface Warfare Center, Carderock Division (NWCCD) took on the role of leading the scaled physical model wave basin testing.

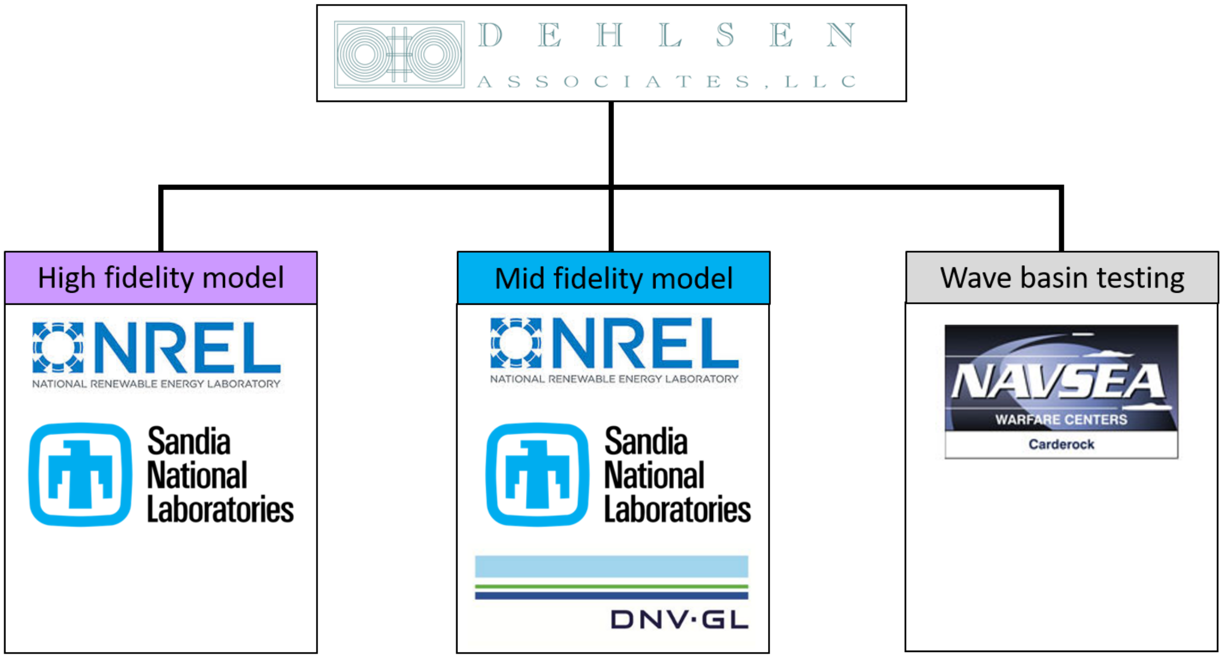

Figure 2 - Project working partners

5.0 Project Task Activities

5.1 Task 1: Establish baseline design requirements

To begin work on Task 1, Dehlsen Associates worked with the national labs and DNV-GL to establish the environmental parameters definition. This defines the sea states to be included for analysis in this project. The DOE LCOE reference resource of Northern California near Eureka [4] was selected as the site with the 100-year contour selected over the 50-year to result in a more conservative design.

The 100-year wave contour for the site is shown below with the sea states of interest for two different extreme conditions investigation approaches: full-sea state and contour.

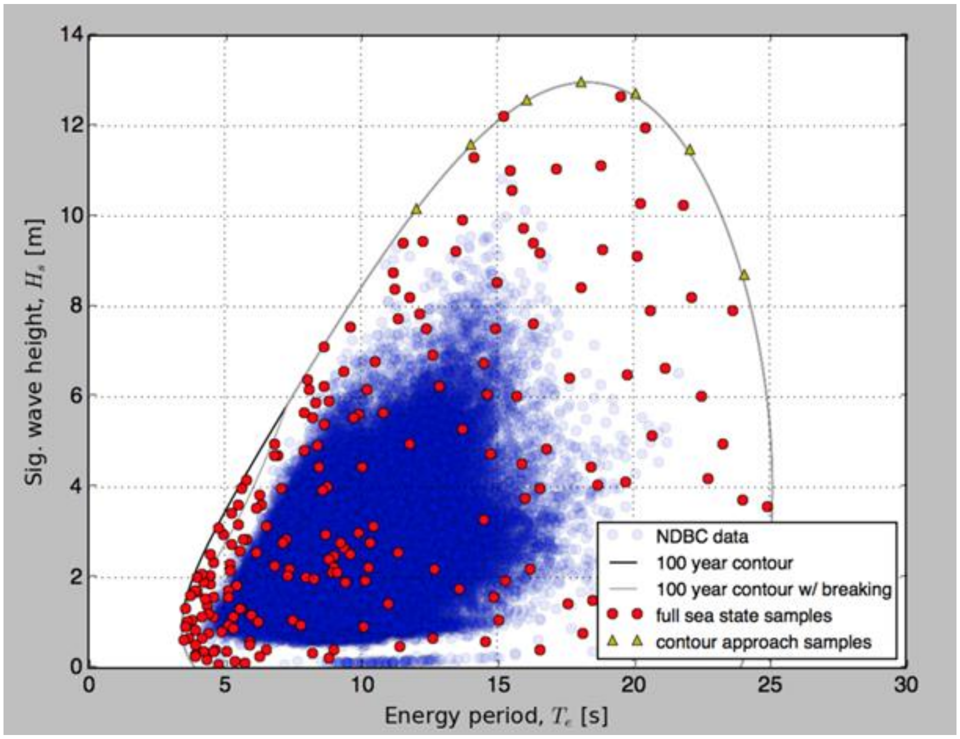

Figure 3 - Eureka 100-year wave contour

As can be seen in the figure, the contour approach features far fewer sea state samples, while the full sea state approach is much more in-depth and includes more cases of study. Analysis of these extreme conditions for consideration in this project was conducted using WEC Design Response Toolbox (WDRT) developed by Sandia National Laboratories and NREL [5]. The full sea state approach thus results in a more robust method at the cost of far more computational time.

The methodology envisioned for this project's mid-fidelity analysis is shown in the diagram below:

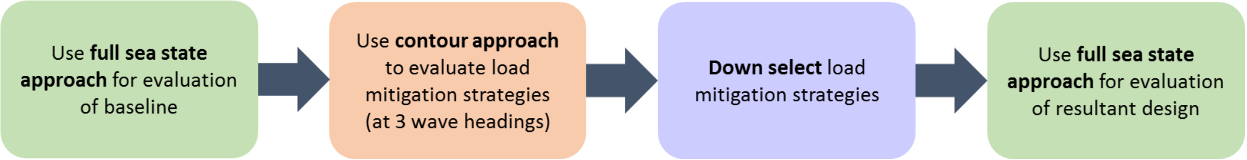

Figure 4 - Original sea state selection methodology plan

Following this plan, and upon the completion of the updated mid-fidelity model in WaveDyn, described in detail as part of Section 5.6 *Task 6: Mid fidelity modeling of WEC*, a full sea state approach was to be used to analyze the baseline configuration with no load mitigation strategy applied. The results of this work would be used not only to create baseline loading conditions, but also to tailor a contour approach for the load mitigation trade study. The trade study was designed to employ the contour approach, which is less computationally demanding and sufficient for the purposes of relative loading between load mitigation cases. However, a contour approach was eventually implemented for both stages of this study rather than using the full sea state approach for the initial baseline.

The load mitigation strategies planned for investigated in this work are shown in the figure below:

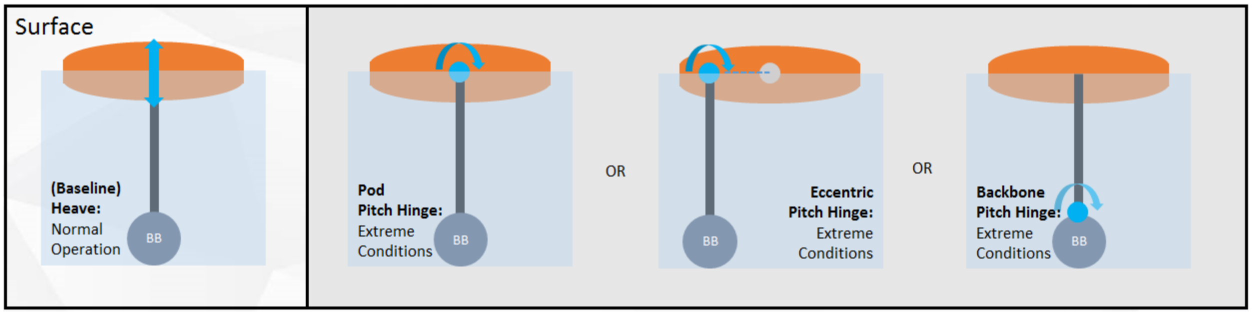

Figure 5 - Load mitigation strategies

Following the trade study, described as part of Section 5.2 *Task 2: Improved WEC design*, the load mitigation strategy resulting in the lowest loading was selected and carried forward into a resultant study.

In order to complete the baseline and load mitigation trade study, updates to the mid-fidelity (WaveDyn) model were required. An existing numerical model of the Centipod WEC built for performance modeling in operating conditions was adapted for use in this extreme condition work by adding PTO end stops and including instant hydrostatics to the model.

End stops added to the model to allow for a more realistic assessment of loads in large waves compared to unconstrained motion (designed stroke depicted below). The constraints on the PTO stroke and associated end stop mechanical properties are provided via an external .dll with an easily editable input file that can be used to study various end stop parameters, including mechanical stiffness and damping.

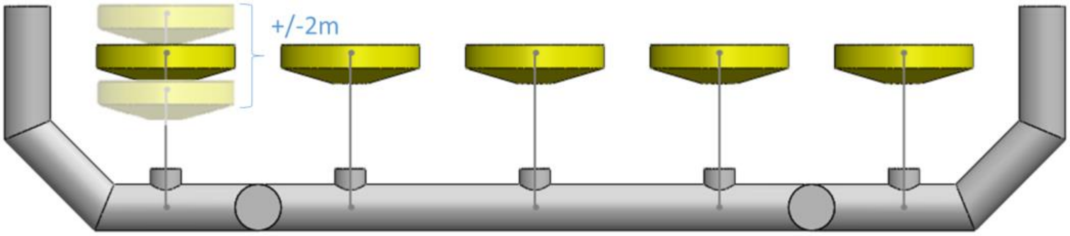

Figure 6 - Heave degree of freedom stroke limit (note: early-project 5-Pod 'Centipod 5P-9' shown[1])

Instant hydrostatics and instant Froude Krylov (FK) forces were added to account for the variance in water line on the Pod bodies encountered in large seas. Application was attempted on all 5 Pod bodies, as well as on the center Pod (Pod 3) only. It was found that both models yielded similar

---

[1] LCOE optimization in parallel with this project resulted in a change from the 5 Pod, 9m diameter 'Centipod 5P-9' WEC design variant to the 3 Pod, 15m diameter 'Centipod 3P-15' design variant early in the project. This design change had cross-over scope with Task 2, and therefore a description can be found in Section 5.2. Original figures from the project are included which represent the state of the WEC at the time of the task reflecting the accurate nature of the WEC's design evolution. The survival methods and other technical attributes of this project are applicable to both design variants but work exclusively focused on 'Centipod 3P-15' after the initial project phase.

results for smaller waves, and the minimum and maximum loading were also similar for large sea states in both cases. The kinematics were slightly different for the large sea states; the model with all floats utilizing instant hydrostatics rolls more than the Pod 3 only case. However, the computational time is four times faster for Pod 3 only. This was chosen as the method for the baseline and load mitigation analysis since the primary concern is a relative approximation of loads between load mitigation strategies. Furthermore, load and kinematic analysis is refined through high-fidelity and physical models later in the project.

Instant hydro	Instant FK	CPU/Simulation time	CPU time [s]
POD3	POD3	5x	4982.506
All PODS	ALL PODS	21x	21083.629

Table 1 - Computation time comparison

Following the completion of the model updates, baseline analysis was initiated revealing further issues with simulation speed.

Slow simulation speeds were encountered when conducting spot tests on several large sea states prior to a full set of baseline states. This was partially due to large waves causing the pods to reach the end stop condition frequently, thus causing the simulation timestep to decrease when the additional end stop mechanical stiffness and damping were added, and the pods experienced a resulting step change in acceleration. Additionally, the combination of the frequent application of end stops and the tension leg mooring system resulted in more severe backbone pitch than initially anticipated. Large response in the backbone pitch and heave degrees of freedom resulted in slack mooring line conditions, further complicating the simulation and slowing the model run.

The challenges surrounding the slow simulation speeds described above have been explored. WEC structural modification was addressed and outlined in the Task 6 write-up. Meanwhile changes to the modelling approach were discussed with DNV-GL to reach a solution to the slow simulation speed including:

- Reducing number of coupled hydrodynamic bodies
- Multiple end-stop stiffness and damping zones
- Reducing number of frequency components in sea state files
- Running large baseline batch (1000 runs) on DNV-GL servers

These changes, in addition to those outlined in Task 6, resolved the computation speed issue in preliminary results. However, when the model was presented with wave headings other than unidirectional broadside to the device, large non-real yaw rotations were observed. This issue led to an extensive period of troubleshooting, leading to the implementation of a better representation of backbone drag as a function of rotational velocity (i.e. yaw damping).

Morison elements were added to the backbone to approximate drag on the structure.

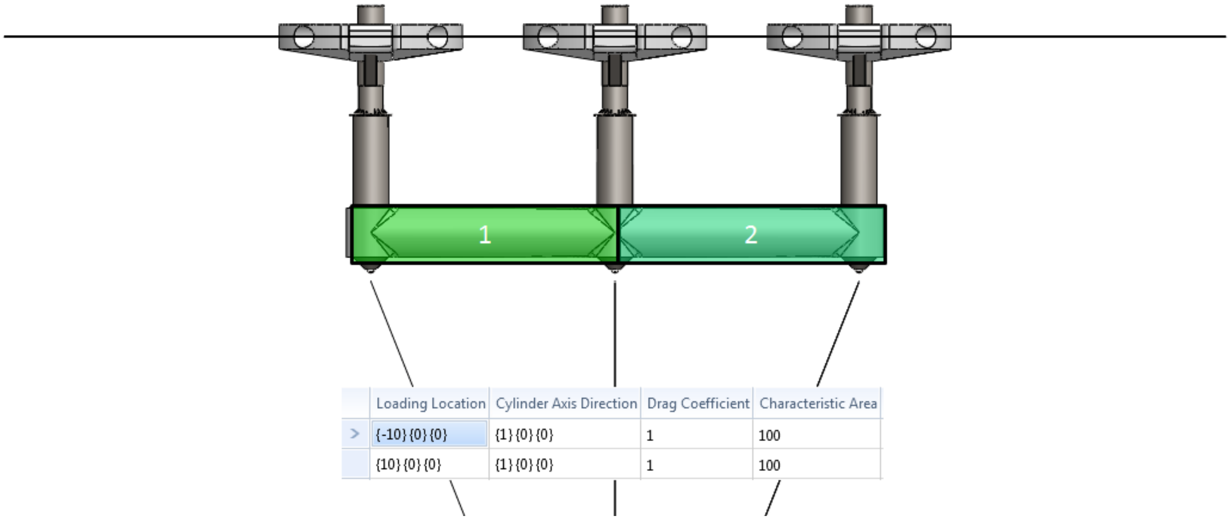

Loading Location	Cylinder Axis Direction	Drag Coefficient	Characteristic Area
{-10} {0} {0}	{1} {0} {0}	1	100
{10} {0} {0}	{1} {0} {0}	1	100

Figure 7 - Two Backbone Morison Elements (note: 'Centipod 3P-15' shown)

This yielded a more stable kinematic response of the structure in large oblique waves. An example time series is shown in the figure below. This example uses ACE Sea State 3 (Hs 5.36m, Tp 11.52, heading -70 deg) [6] as it is a fairly large sea state with a wave heading far from the ideal broadside case, and thus likely to cause significant backbone yaw.

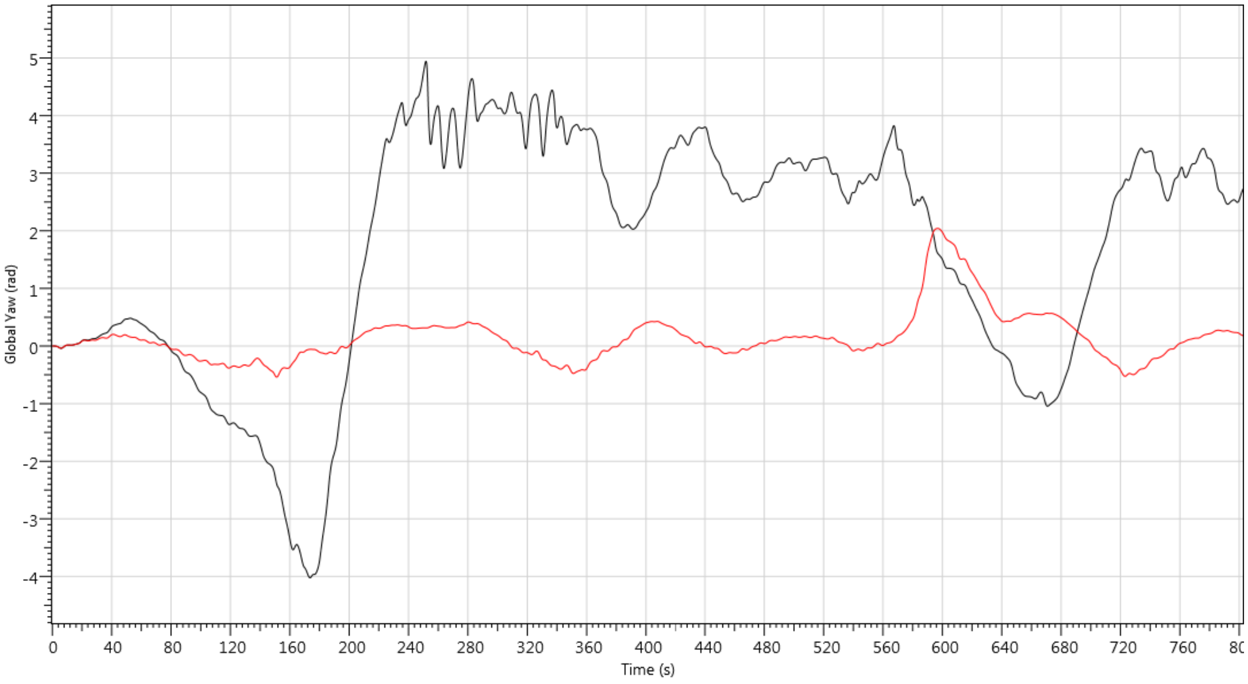

Figure 8 - Two Backbone Morison Elements (red) vs. No drag component/damping applied to Backbone (black)

The figure above shows that without damping applied to yaw rotation, the model produces what are likely non-real results. When the two Morison elements are applied to the backbone, the yaw motion was much more stable and closer to what is expected of the WEC kinematics.

In addition to adding Yaw rotation damping through the method described above, DA also increased the mooring line pretension in an effort to reduce the chance of loss of model stability due to slack mooring conditions.

Following an extensive process of refining the numerical model for use in a load mitigation trade study, the model was ready for use. The numerical model was used to evaluate multiple load mitigation strategies under extreme conditions leading to comparison of load shedding modes, but was limited to the contour approach, a limited sampling of sea states on the 100-year curve, rather than the original aspiration to conduct the trade study using the full sea state approach. This decision reduced computation time from a matter of months to matter of weeks.

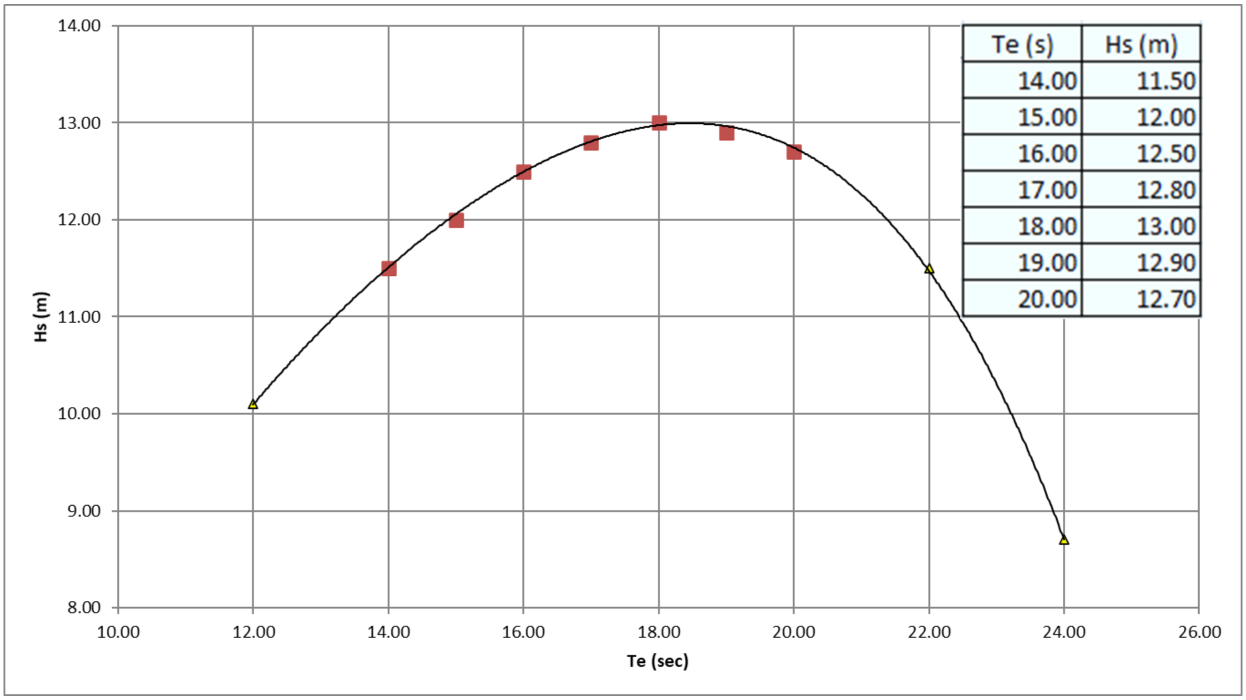

Te (s)	Hs (m)
14.00	11.50
15.00	12.00
16.00	12.50
17.00	12.80
18.00	13.00
19.00	12.90
20.00	12.70

Figure 9 – Trade study sea states selected on 100-year contour

5.2 Task 2: Improved WEC design

Work on the WaveDyn model as part of Subtask 6.1 was undertaken in Q2 2017. It was originally planned for the model to be updated after a full baseline extreme event set had been modeled. However, preliminary results from the numerical model were suffering from slow computation times which were partly due to erratic kinematics of the Wave Energy Converter in very large waves. To alleviate this problem the structure of the WEC was modified with a primary focus on increasing the depth of the backbone, shortening the backbone, increasing pod diameter in a three-pod configuration, and moving to a mooring arrangement with fewer lines that was less prone to slack conditions. This design improvement was combined with an ongoing LCOE based design improvement to result in the new ‘Centipod 3P-15’ design variant.

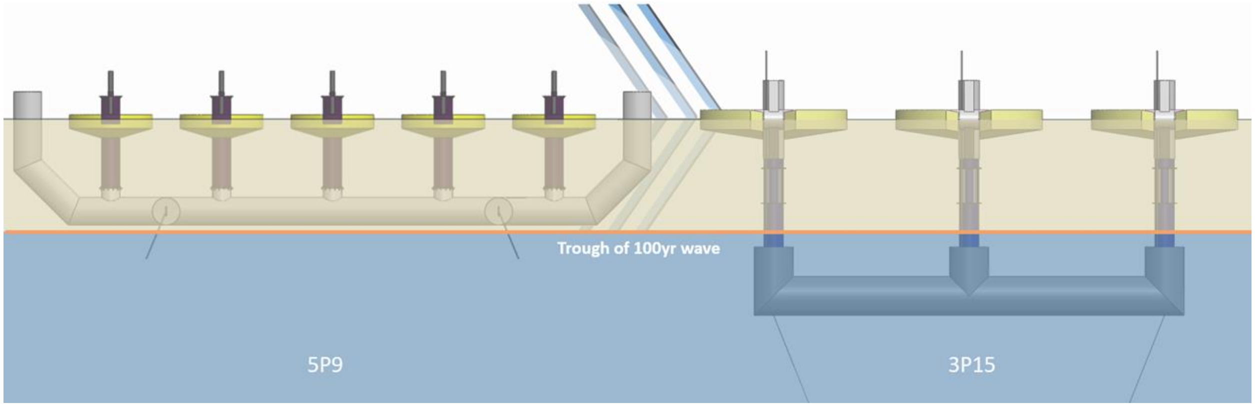

Figure 10 - Design transition from 5P-9 to 3P-15

Structural changes to the WEC in the WaveDyn model were implemented, resulting in a new, more functional numerical model.

Work continued on the evaluation of load shedding methods by comparing numerical model data between the baseline configuration and load shedding configurations incorporating additional degrees of freedom.

5.2.1 Survival Design Down-Selection

A critical step within this project was the definition of a mechanical method of load mitigation for Centipod, the survival design down selection. This effort was undertaken using the mid-fidelity model of Centipod as described previously.

With the tools in-hand, the effort began by defining two important criteria. The first criteria was the selection of design loads to be evaluated. Wave energy converters are subject to very complicated load-sets due to their operating environment, and loads could be evaluated at any number of positions on the WEC, but in order to simplify the down-selection process a small number of critical load cases had to be used to easily compare different load mitigation methodologies. The three load cases under careful examination in this effort were the following:

1) Mooring Line Tension
2) Axial Force at Pod-spar/ backbone junction
3) Pitch moment at spar base

These primary design load cases were selected because they have significant impact on the capital expense of the structure. The figure below gives a visual representation of these load cases on the WEC model.

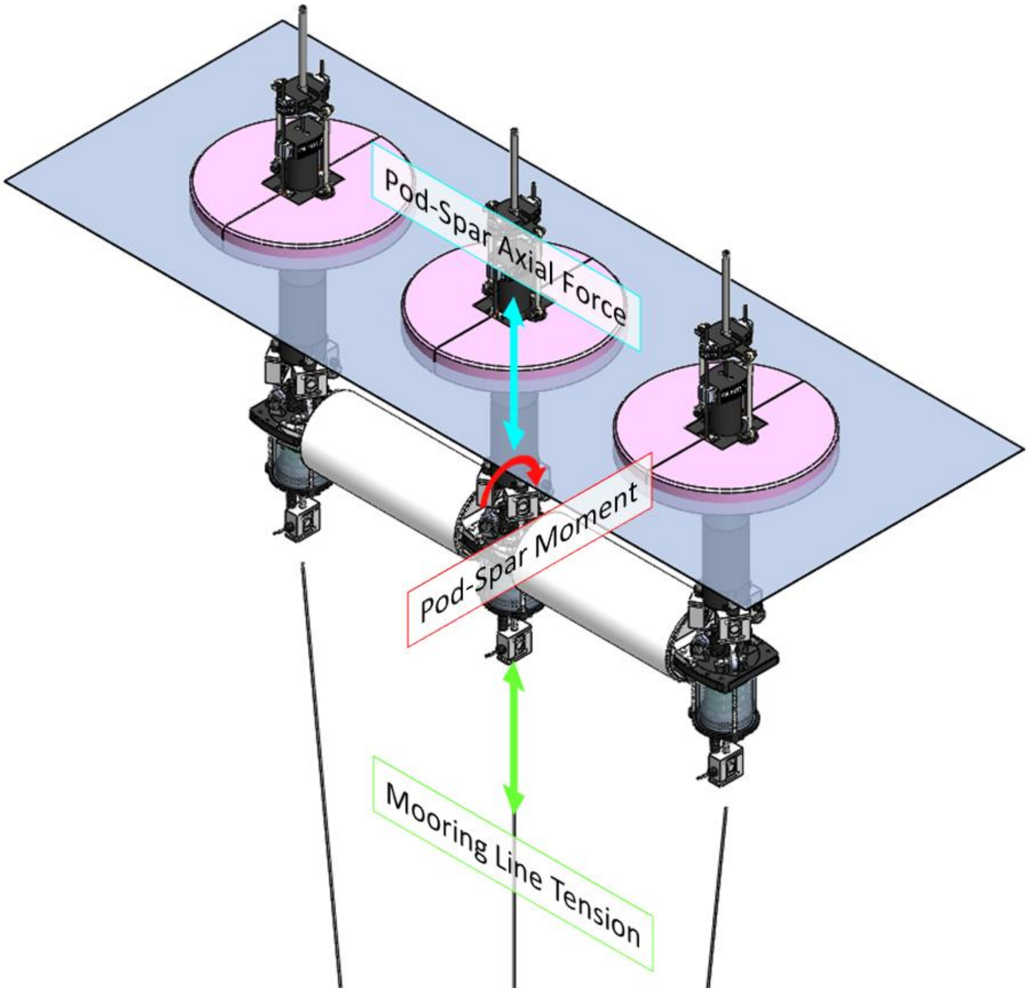

Figure 11 - Primary load cases

The Pod-Spar axial force and bending moment combine to lead to the structural requirements for the Pod-Spar, which transmits all Pod loads from the Pod to the backbone and moorings, and also houses the power take-off with associated electrical equipment. Decreased moments or axial loads will result in a decreased wall thickness of the tubular structure and reduced system capital expense (CapEx). Meanwhile, the mooring line tension affects the CapEx of not just the mooring lines themselves, but more importantly every aspect of the mooring system down to the piles. The effects of maximum mooring line tension extend beyond CapEx as pile size will determine the type of vessel required for installation, causing an Operations and Maintenance (O&M) as well.

The second major criteria to be established in this trade study was the determination of the load mitigation strategy candidates themselves. First, the high-level nominal strategies needed to be established. This was easily done as the original proposal called for an investigation into “feathering” methods which in essence require an additional rotational degree of freedom. If this notion is expanded slightly the additional rotational degree of freedom used in feathering can also be used for a physical transformation that occurs in a transition phase then is left with the static resulting transformation throughout extreme events. Since this utilizes the same notion of an additional survival degree of freedom but remains static throughout the event, it was nominally re-classified as "folding" for clarity's sake. The nominal methods to be explored then include:

1) Baseline
2) Feathering
3) Folding

Of these nominal methodologies, several parameters are available for alteration which affect the performance of each nominal method. For example, the baseline could be heave-locked, or free to heave with the operational stroke. The feathering hinge could be set to rotate about the Pod centroid, or an eccentric axis, and the hinge could operate in tandem with the heave degree of freedom or not. With respect to the folding method, the fold could rotate the hemispheres either up or down. Some simple analysis could be done to get a good picture of the prospects of some of these options, for example, the up verses down fold options are examined in the figure below.

Assuming a 4m stroke, the folding action would:

On Fold Up:

a) Move the pod core down 2m [2]
b) Fully submerge the core and portions of the hemispheres
c) Result in ~20% submergence below still water line (SWL)
d) Raise the center of mass (COM) higher on Pod-Spar

On Fold Down:

a) Move the pod core up 2m
b) Submerge most of the Hemispheres
c) Result in ~90% submergence below SWL
d) Lower COM on Pod-Spar

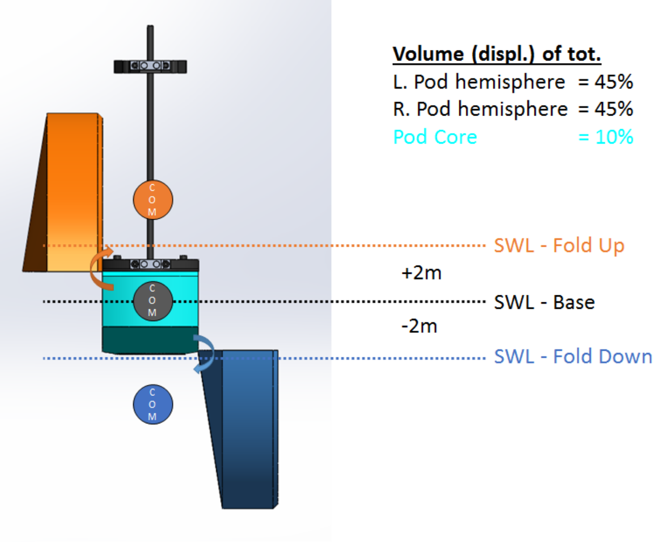

Figure 12 - Comparison of up versus down fold

This simple geometric analysis gave some confidence that folding down may be a marginally better solution since there was a lower pod center of mass. The hydrodynamic impacts of the down fold may have offset this, however so it was worthwhile to check this hypothesis and all others in a simple pre-select of the nominal load mitigation methodologies. A pre-screening of different options within the nominal methodologies was carried out to refine the design of these survival methods. The best parameters could then be selected for the more detailed trade-study comparing baseline, feathering, and folding.

A comparison between a selection of numerical model results is shown in the table below.

---

[2] The mechanism designed to fold the Pod requires an opposite translation in the core with respect to the hemispheres.

Survival Mode			Maximum Absolute Value				
Class	Main Parameter	Secondary Parameter	Mooring Ln 1 Force (MN)	Mooring Ln 2 Force (MN)	Mooring Ln 3 Force (MN)	Axial Force (MN)	Pitch Torque (MNm)
Baseline	-	No Heave	12.373	12.373	12.372	7.996	11.486
Baseline	-	4m Heave	11.466	11.466	11.466	6.960	13.043
Feather	Non-Eccentric Pitch Hinge	No Heave	20.352	18.431	18.011	13.208	24.551
Feather	1m Eccentric Pitch Hinge	No Heave	18.056	18.056	18.055	12.160	17.597
Feather	5m Eccentric Pitch Hinge	No Heave	13.141	13.129	13.117	8.597	56.130
Feather	5m Eccentric Pitch Hinge	4m Heave	12.842	12.856	12.870	10.750	64.851
Fold	Folded Up	No Heave	6.610	6.684	6.758	4.077	1.638
Fold	Folded Down	No Heave	6.147	6.182	6.280	3.333	2.427
Fold	Folded Down	4m Heave	6.082	5.786	5.883	3.133	2.157

Table 2 - Selected numerical model result for different parameters within the nominal families

Generally, the allowance for operational heave with the 4m stroke limit did not result in much improvement to loads in the baseline or the two load mitigation configurations. This is logical; the 100-year wave heights can be up to five times larger than the operational stroke, rendering it insignificant in these extreme cases. The lack of clear evidence for a benefit coupled with the challenges of accurately modelling the end stops (in both the numerical model and the physical model) led to the conclusion that heave would be fixed for extreme condition analysis.

Similarly, the pre-screening showed consistent evidence that eccentric hinges, which are slightly beneficial for mooring line force reduction, drastically increased the bending moment in the Pod-Spar structure.

Finally, the downward folding direction was confirmed to have a slight edge over the upward folding option in this initial analysis. Both directions had favorable results, however, and credible design solutions may exist for either option.

Following the refinement of nominal load mitigation methods, the three options were taken forward into more extensive numerical modelling with each design variation being modelled and simulated for each of the contour sea states.

As a visual example of a time series simulation result comparing a baseline to a load mitigation method under the same simulated event, the figure to the right is provided.

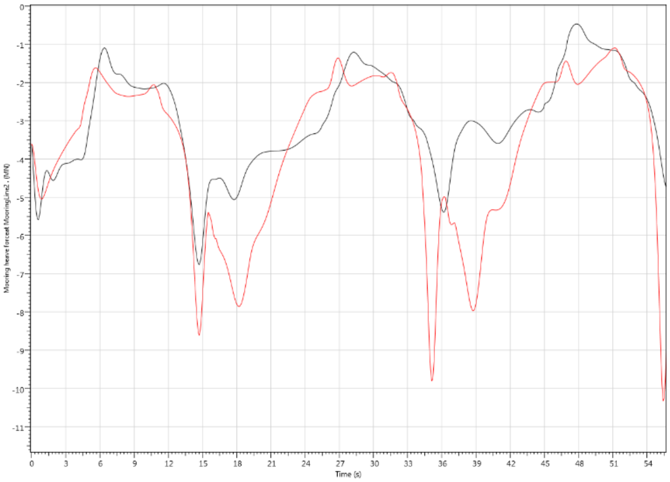

Figure 13 - Example load time series of baseline (black) a load mitigation method (red) under the same simulated event

Because the output loads time series were not a simple harmonic, identifying ultimate loads as single points and comparing those ultimate loads proved to be inadequate for this trade study. Instead the probability of a peak load occurring was compared.

To begin this analysis, each load time series was filtered to identify the peaks using the WAFO toolbox for MATLAB [7].

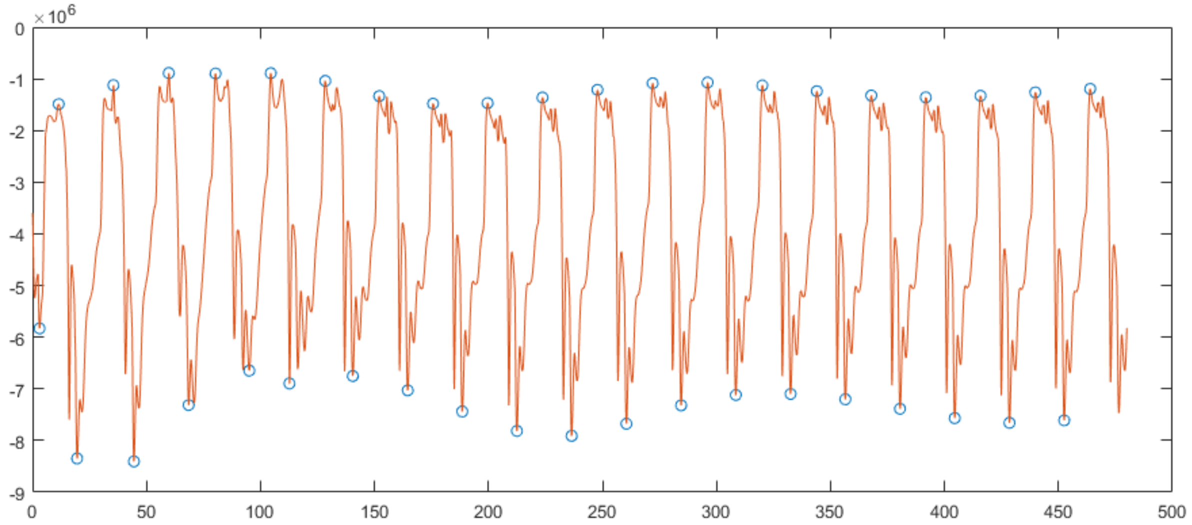

Figure 14 - Peaks identified within time series

With the method of peak selection refined and checked, it was then possible to process the raw time-series data from the mid-fidelity simulations of each nominal design under each of the 7 100-year contour wave conditions.

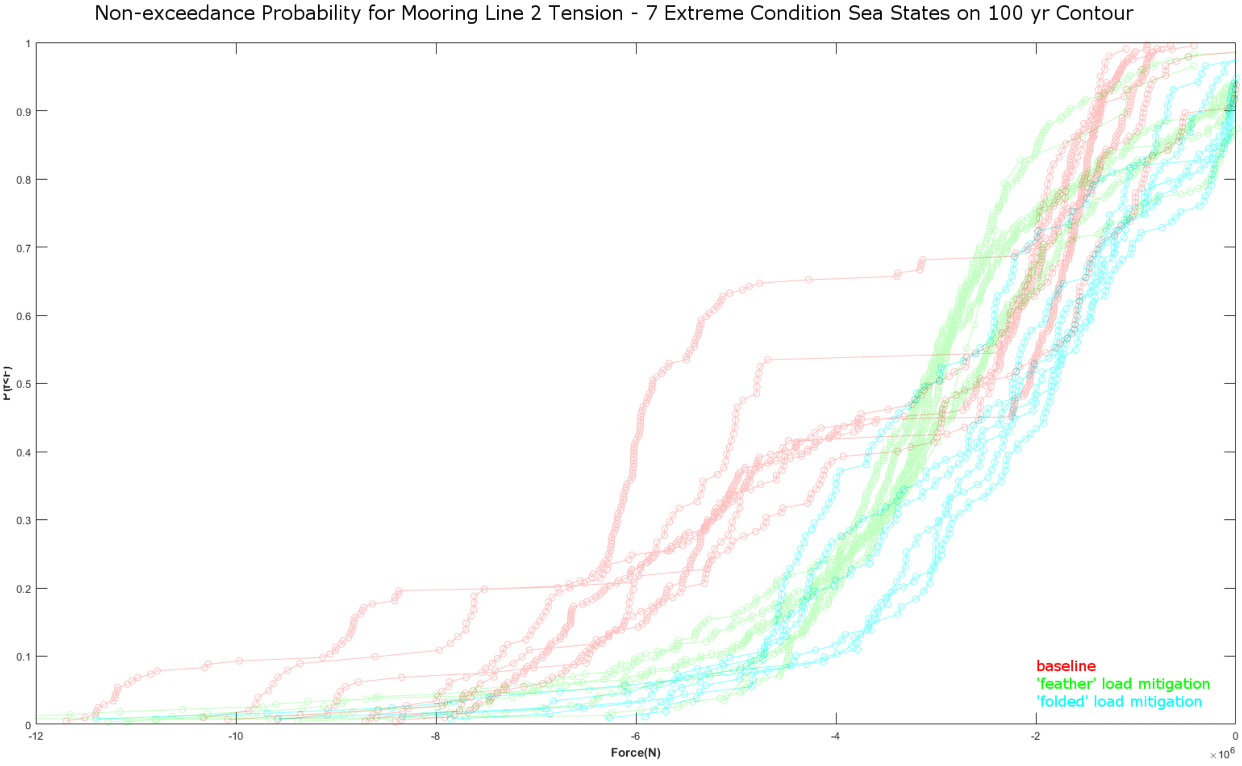

Figure 15 - Individual plots for each of the 7 repeated regular 100-year waves

These results were combined into unified probability curves for each nominal design for each loading condition for comparison.

Each run of multiple regular wave period showed variance between peak loads each wave despite identical excitation from each wave. While some variance could be attributed towards device kinematics and momentum of the physical bodies brought from one cycle towards the next, there was a noticeable trend of outlier data points occurring. As a result, analyzing numerical model data was less straight-forward than anticipated, and ultimate loads were compared at 95% probability level to filter out possible non-real outlier data points. The resulting non-exceedance plots are shown in the figures below.

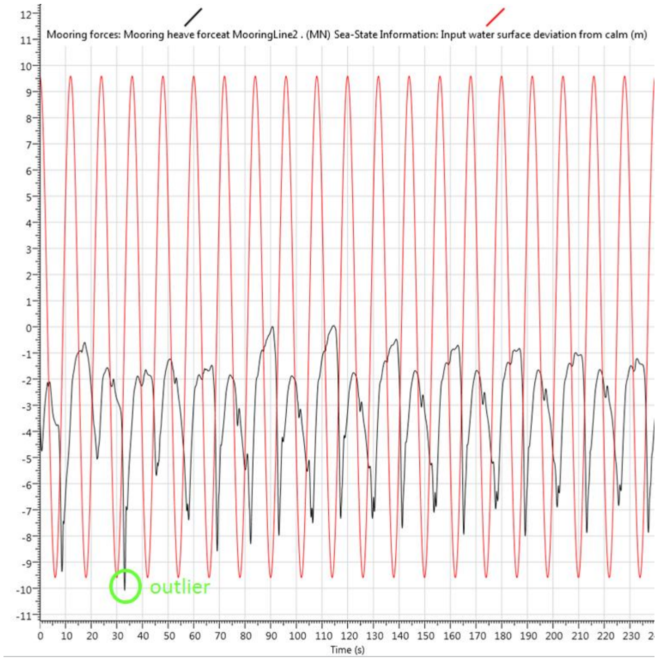

Figure 16 - Example of mooring line tension output time series in a regular wave

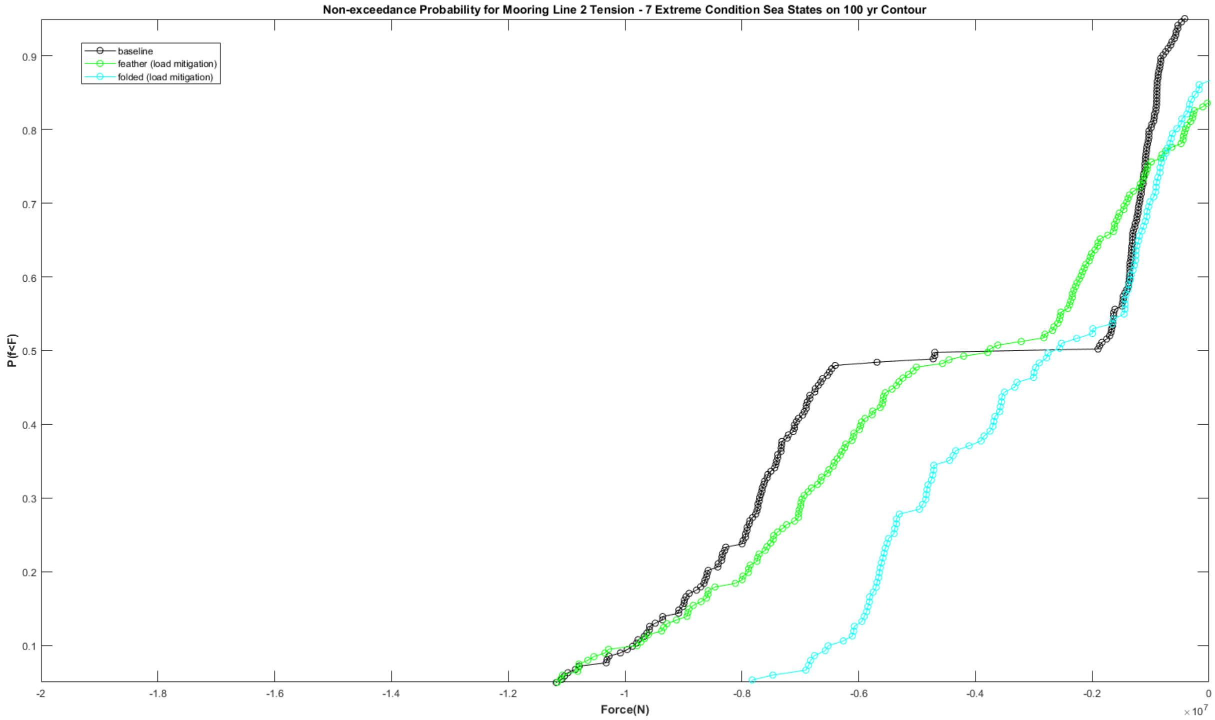

Figure 17 - Mooring tension non-exceedance plot for combined data from 7 regular waves on 100yr contour (each regular wave repeated at least 10 cycles), y axis 5 – 95% limits

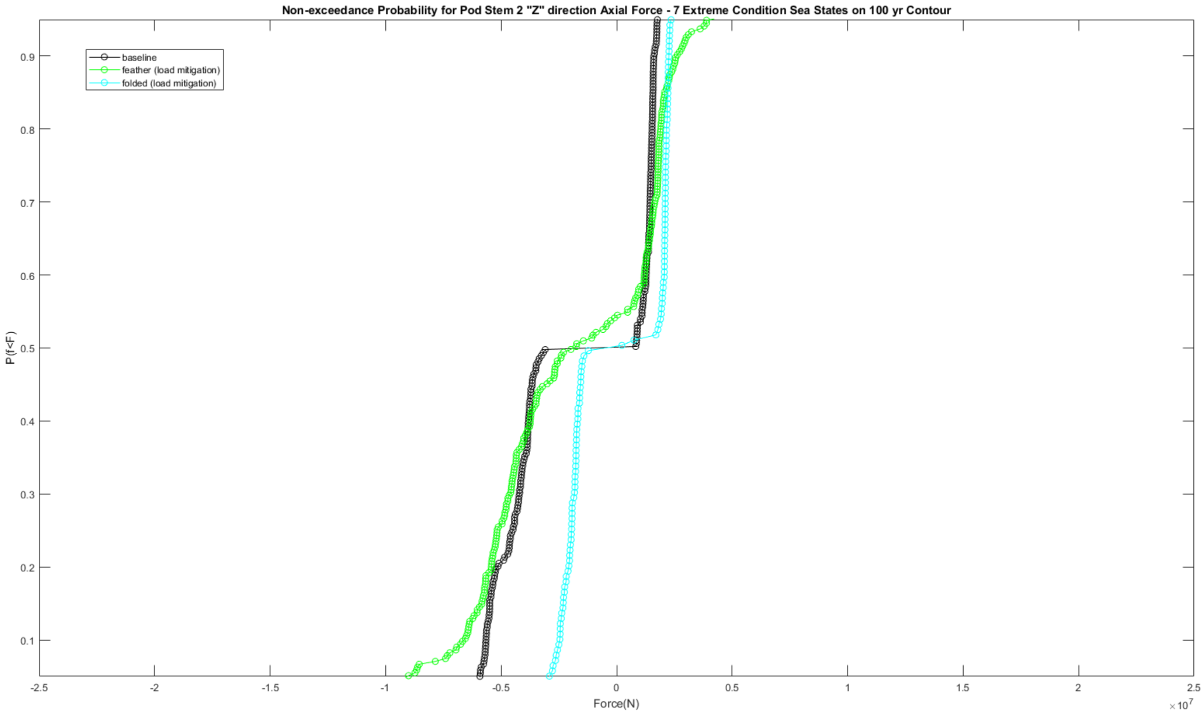

Figure 18 - Axial force at Pod stem 2 non-exceedance plot for combined data from 7 regular waves on 100yr contour (each regular wave repeated at least 10 cycles), y axis 5 – 95% limits

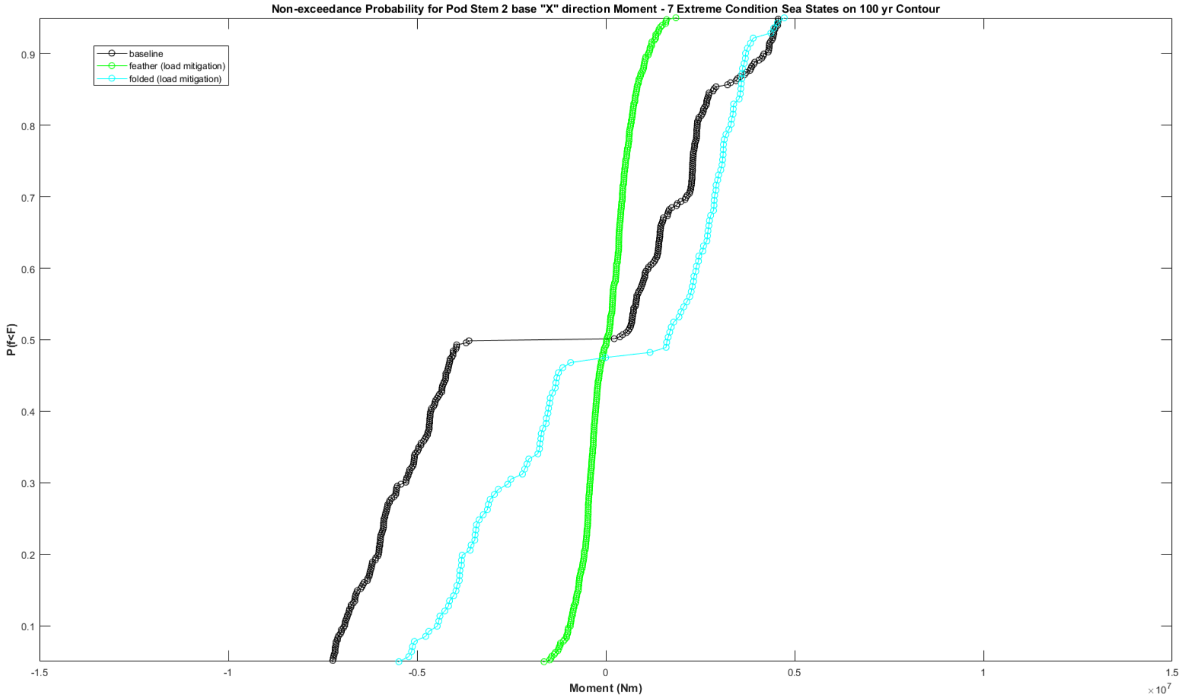

Figure 19 - Moment about X axis at Pod Stem 2 base non-exceedance plot for combined data from 7 regular waves on 100yr contour (each regular wave repeated at least 10 cycles), y axis 5 – 95% limits

The results of this down-selection investigation confirmed the preliminary results that showed the folding load mitigation method to be desirable compared to the feathering method. The feathering method showed similar results to the baseline in maximum mooring line tension, while performing worse than the baseline in axial force. Meanwhile, the folding method showed promising results in both load cases. As a result of this work, the folding load mitigation method was selected to move forward into physical model testing.

5.3 Task 3: Design scale WEC model for test

The basin scale model WEC design began with assessment of the wave maker capabilities at the test facility. Shown below is a draft assessment of the Naval Surface Warfare Center maneuvering and seakeeping (MASK) basin’s wave maker capabilities. Wave maker limits are shown in the upper right legend and overlaid with the maximum possible waves to be tested at model scale as defined by the 100 year wave contour utilized in this work, these are shown as dotted lines in lower right legend.

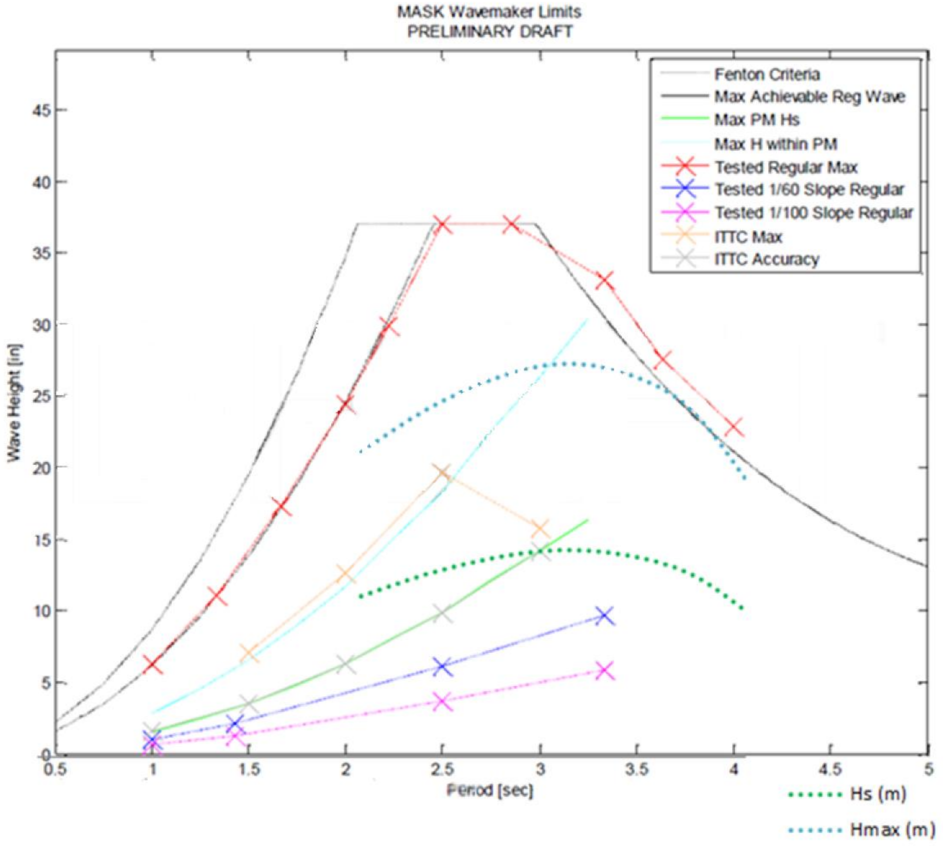

Figure 20 - Wave maker limits versus waves required for 100-year contour at scale

The model scale was set to the largest possible scale within the wave maker limits.

Once the scale was determined, and in parallel with Task 2, the design of the scale model WEC began with preliminary mechanical designs and layout of sensors. This allowed the team to evaluate conceptual designs of the scale model in parallel with the down select process. For example, shown in the figure to the right is an early conceptual model of the eccentric hinge "feathering" design option with a reversible hinge axis. This early consideration allowed the team to hit the ground running with the design choice eventually emerging from the down-selection process.

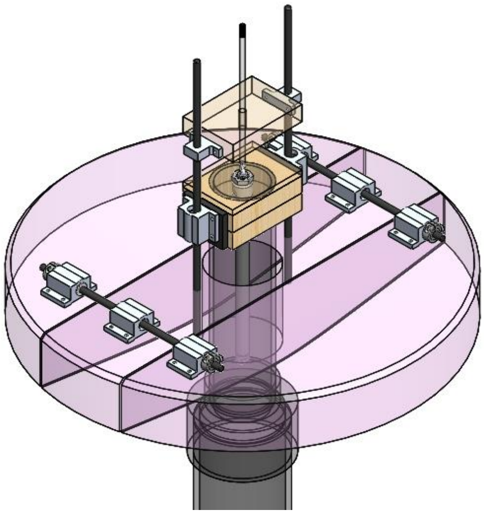

Figure 21 - Early conceptual model of eccentric hinge model deisgn

Once the folded design choice was made, the design options for the scale model were weighed to establish a practical model that was representative of the full-scale WEC design and achievable on small scale. Manual folding action was determined to be adequate for wave basin testing since it would only need to be carried out intermittently between tests. However, a mechanism was still needed to allow a manual transition and reliable hold of the Pod geometry in either folded or non-folded orientation. The design process was iterative and included some hydrodynamic consideration for variances in the size and shape of the Pod "core".

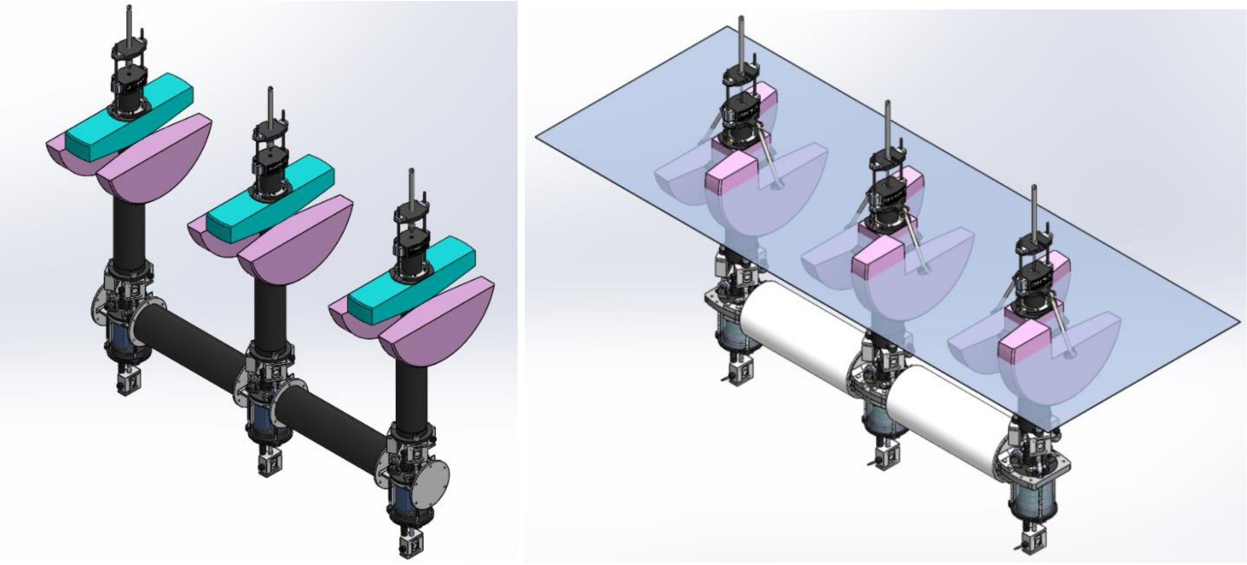

Figure 22 - Early design evolution of the downward foolding model mechanism

Meanwhile, the preliminary layout of sensors and instrumentation was established to allow for a better understanding of the mechanical interfaces between the components and the instruments. This effort also went through several iterations as the down-selection process was conducted and in light of practical model-scale design decisions.

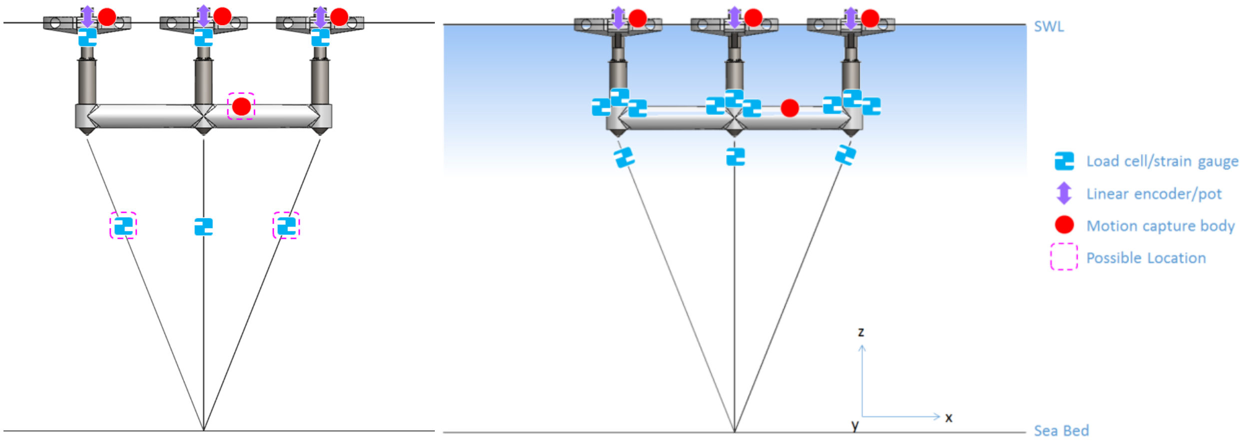

Figure 23 – Early-stage (left) and late-stage (right) sensor layout plans

The combination of an established model scale, instrumentation layout, and load mitigation methodology allowed mechanical modeling and component selection for the model to begin. Of primary importance in the design of the scale model was the load cell array that would be used to collect data on axial loads and bending moments in the Pod-Spar, as well as tension in the mooring lines.

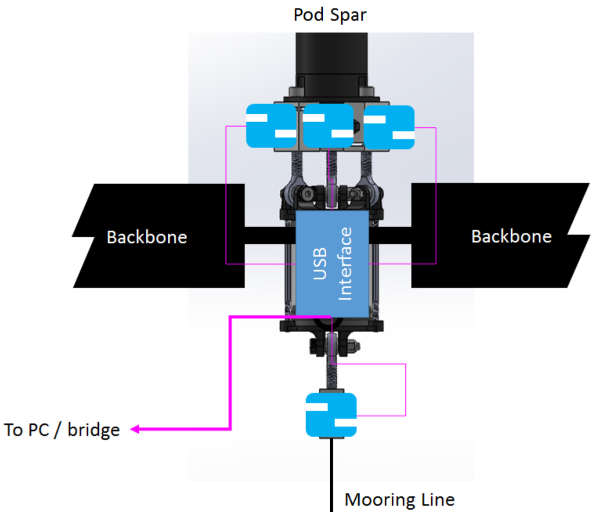

Figure 24 - Prelimainary layout of laod cell array

The load cell array shown in the figure above includes 3 load cells at the Pod-Spar connection to the backbone arranged in a triangle 120 degrees from one another. This array of load cells will be used to measure axial force and moments in the pitch and roll directions. The relative tension and compression readings of the trio of load cells at the Pod-Spar base can be used in conjunction with the known spatial geometry of the array to measure the torque in the pitch and roll axis. Additional linear potentiometers were included on the top-side of the Pod to measure the heave displacement. Additionally, a load cell was fixed in-line with each of the mooring lines for measurement of mooring line tension. Finally, 6 degree of freedom kinematics measurement was made available through Navy equipment applied to the completed model prior to testing.

The final design of the model is depicted in the following two figures.

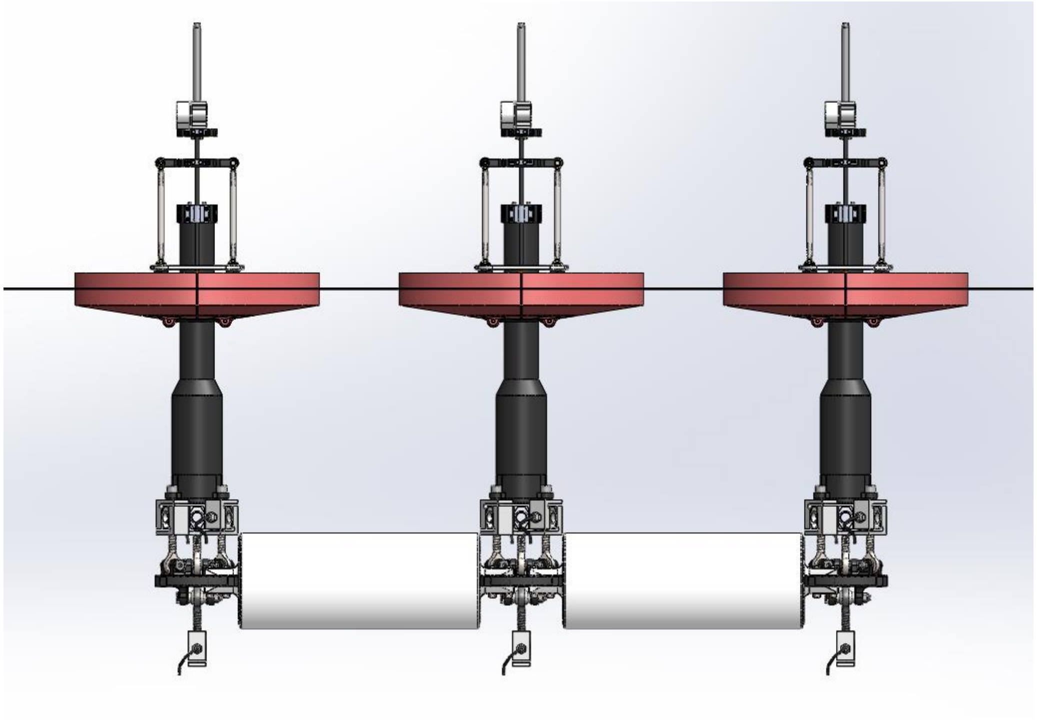

Figure 25 - Final scale Centipod model design, front view

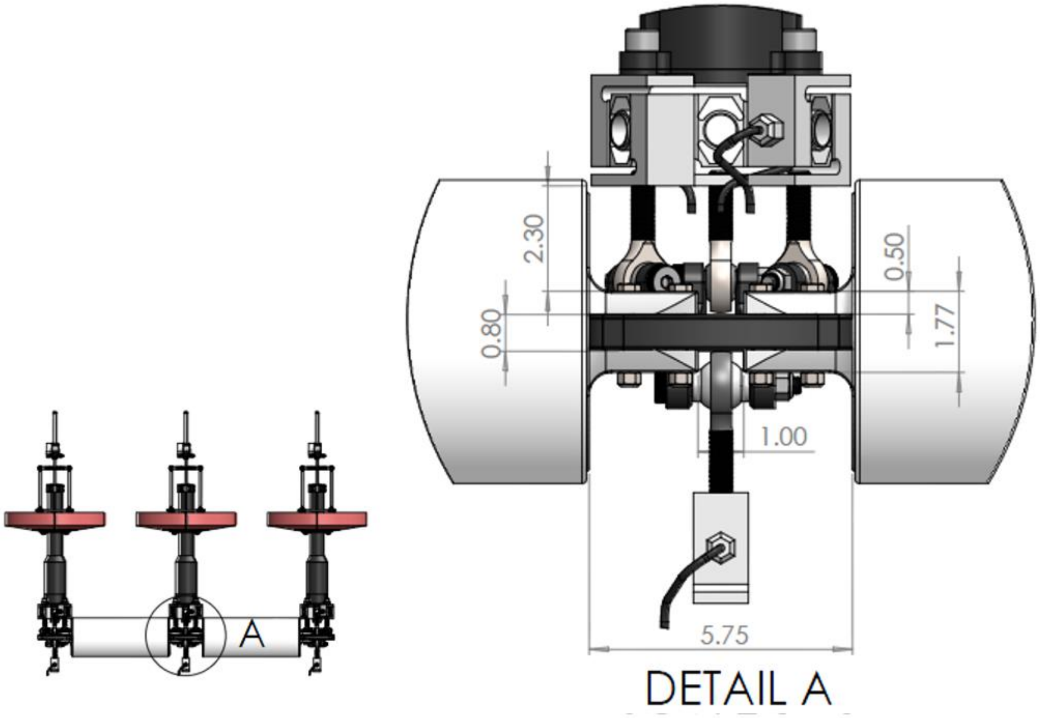

Figure 26 - Main cluster of load cells for Spar axial force, pitch roll moments, and mooring line tension

With the final design of the scale Centipod 3P-15 wave basin model complete, it was possible to move on to the distribution of model geometry to project partners for numerical model refinement, and more immediately, the initial stages of model building.

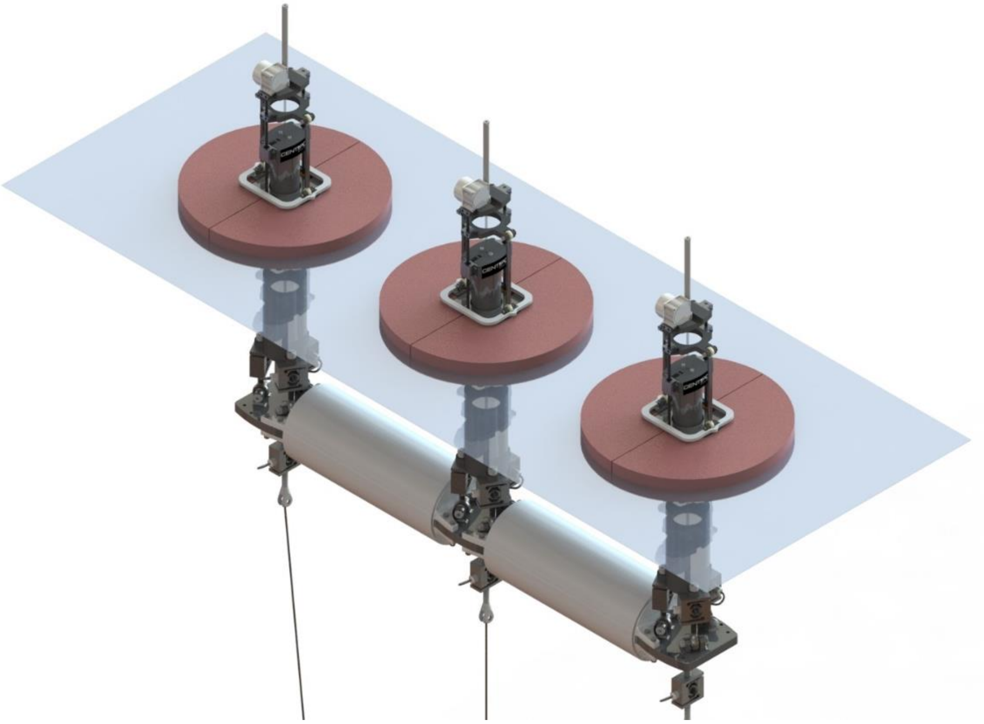

Figure 27 - Final scale Centipod, isometric view

5.4 Task 4: Build scale WEC model for test

The model was broken into 3 subassemblies for design and build: the Pod and Spar combined with the folding mechanism, the sensor array joining the Spar base to the backbone, and finally the backbone segments.

Figure 28 - Pods in fabrication

The Pod and Spar subassembly was the most difficult to build due to having the most specific hydrodynamic geometry in the Pods and containing the relatively complicated folding mechanism. The Pod shape was built by layering a series of high density foam discs cut on a revolved hot-wire cutter and joined into the final shape, then split into hemispheres and coated with a watertight and strong epoxy compound. Prior to the final layer of epoxy, holes were bored into the top of the Pod for the insertion of ballast mass to be permanently integrated within the structure replicating the full-scale design’s scaled mass and center of mass. Threaded inserts were also anchored within the top surface of the Pod hemispheres to allow for attachment of the pinned joint linkage attachments. Similarly, a 3D-printed hinge mount was integrated with the lower side to accommodate the lower pinned joint. Space for the Pod core was removed from the hemispheres as the Pod core was fabricated separately.

The folding mechanism and mounts for the linear encoder and linear damper were fabricated primarily using a 3D printer with linkages and joints generally being assembled from off-the-shelf components and bearings. The mechanism on the top-side of the Pod allowed for heave motion as well as folding for subset of operational scale sea state testing for characterization prior to extreme condition testing. The heave slide degree of freedom was incorporated into the folding mechanism, simulating the relative vertical repositioning of the Pod hemispheres and the Pod core as designed for the full-scale WEC. This sliding motion allowed for a convenient method of locking the configurations since clamps were built into the heave slide mechanism that could be tightened after manually switching orientation.

The sensor array was less mechanically challenging than the Pod and Spar, but held its own challenges, as it needed to be detachable from the backbone and Spar for safe transport yet provide a secure connection between the two other subassemblies once joined. This joint also needed to house 4 load cells in close proximity while still allowing for reliable measurement from each. The solution was a 3D-printed plate made of a tough nylon material that allowed for all the required interfaces and their associated load transfer.

Finally, the Backbone segment was the least challenging component. The backbone contained no moving parts and was simply needed for connection and to provide buoyancy for mooring line pre-tension. A standard pipe size was available for the scale Backbone tube diameter, so this was cut to length and fitted with custom 3D-printed plugs to seal the tube and allow for connection to the sensor array.

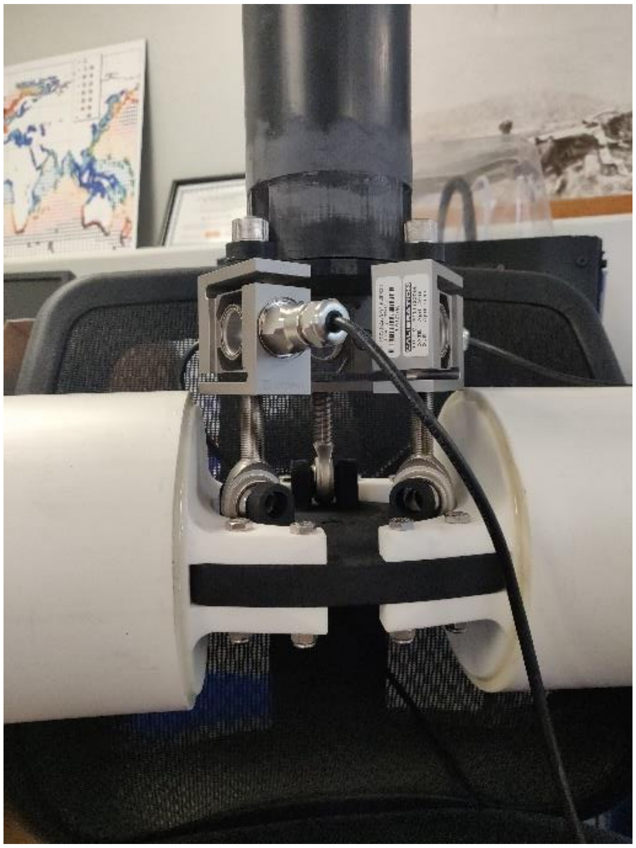

Figure 29 - Sensor array attached to Backbone

The subassemblies were joined and tested for desired buoyancy and sensor feedback in a pool prior to shipping the model to the Navy MASK facility to reduce risk once testing was underway. These preliminary tests of the buoyancy, hydrostatics, and sensor operation went smoothly confirming the model functioned as designed.

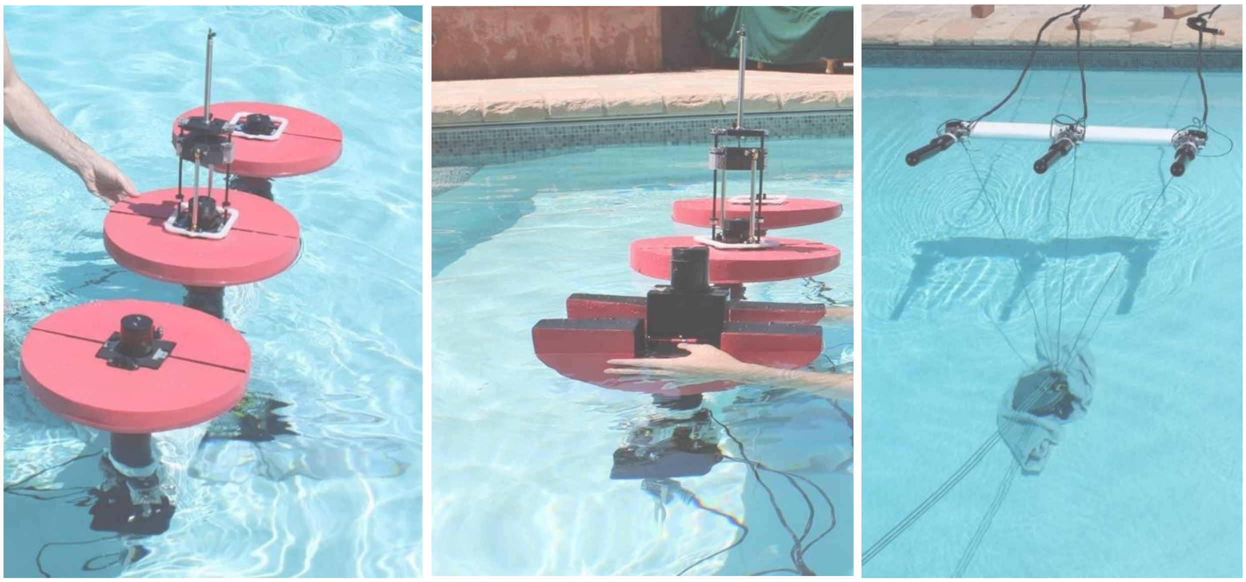

Figure 30 - Testing of model buoyancy and stability (left), Testing "folded" load mitigation configuration (center), Testing of mooring line tensioning procedure without Pods show (right)

After preliminary testing of buoyancy and sensor functionality, the WEC model was disassembled and shipped to the Navy MASK facility for testing.

5.5 Task 5: Wave tank testing

Wave basin testing occurred at the Naval Surface Warfare Center maneuvering and seakeeping (MASK) basin in Bethesda, MD, over the course of two weeks in the summer of 2018. The goal of testing the model scale WEC was to gain data for validation of the numerical models used to evaluation of extreme conditions loads. More specifically, the objectives for testing included:

Figure 31 - NSWCCD MASK Basin

- Moment of inertia testing
- Decay testing for an outer Pod, and the central Pod
- Testing in 8 operational seas, including the set of ACE sea states and two larger irregular seas
- Testing 6 regular waves corresponding to the largest waves on the 100yr contour at two headings

Prior to entering the basin, dry testing of the individual Pod in both baseline and folded configuration was conducted to record the moment of inertia of the model using Navy's moment of inertia testing table.

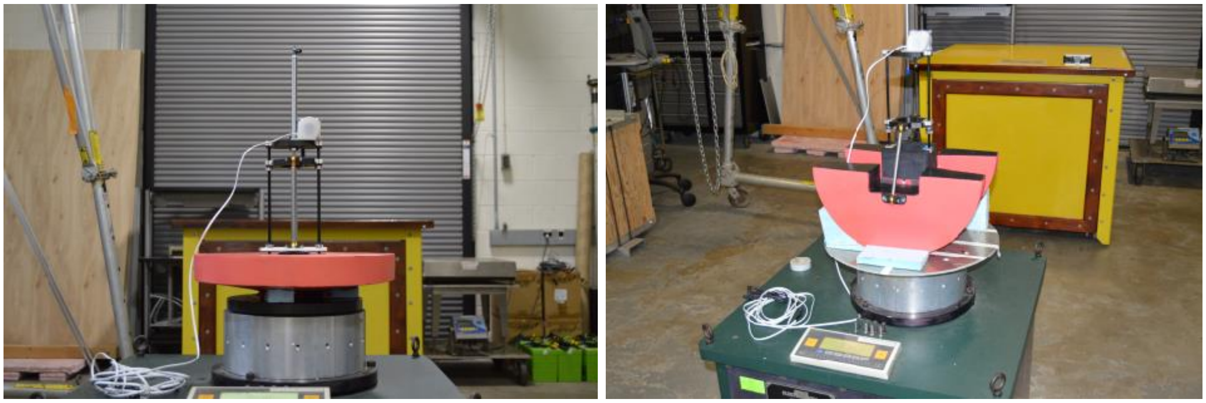

Figure 32 - Moment of Inertia (Yaw) testing in baseline configuratio (left). Moment of Inertia (Yaw) testing in baseline configurationm (right).

Moment of inertia testing was completed on each of the rotational degrees of freedom (roll, pitch, yaw). The superposition principle was used to later add the backbone and spars to the Pod moment of inertia experimental data yielding the full WEC moments of inertia in each configuration.

As discussed in the sections covering the model design and build, the model was instrumented to record data for several key loads for evaluation of the WEC design and validation of the numerical models. The final list of on-board sensors is shown the table below.

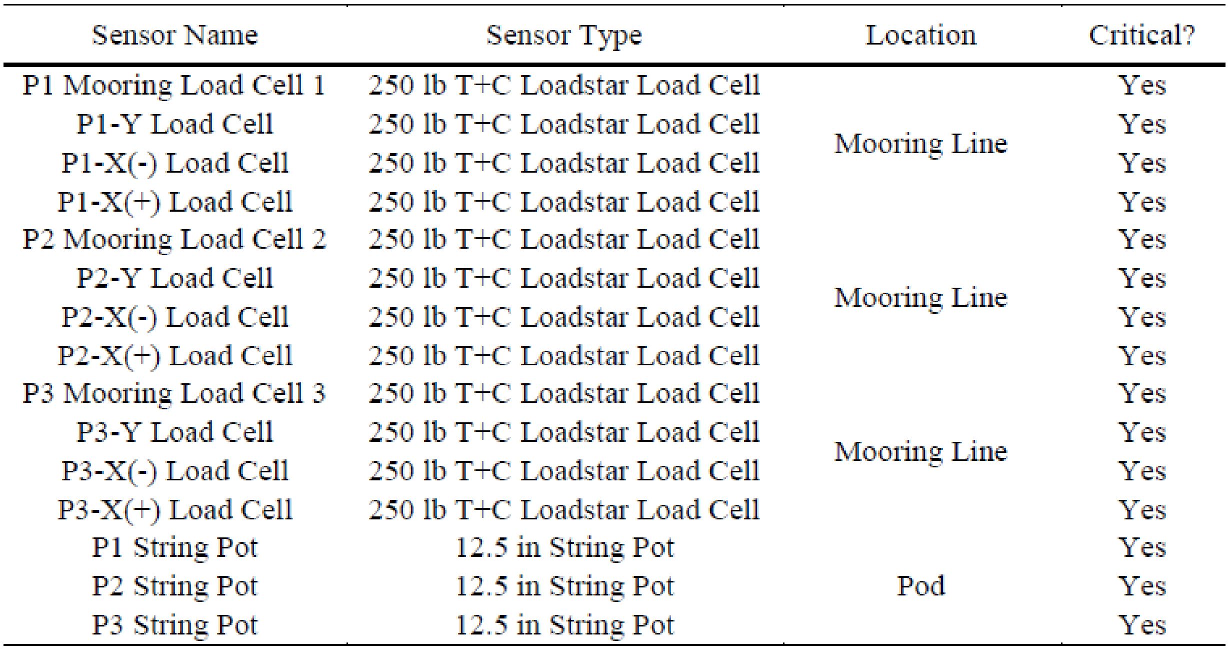

Sensor Name	Sensor Type	Location	Critical?
P1 Mooring Load Cell 1	250 lb T+C Loadstar Load Cell	Mooring Line	Yes
P1-Y Load Cell	250 lb T+C Loadstar Load Cell		Yes
P1-X(-) Load Cell	250 lb T+C Loadstar Load Cell		Yes
P1-X(+) Load Cell	250 lb T+C Loadstar Load Cell		Yes
P2 Mooring Load Cell 2	250 lb T+C Loadstar Load Cell	Mooring Line	Yes
P2-Y Load Cell	250 lb T+C Loadstar Load Cell		Yes
P2-X(-) Load Cell	250 lb T+C Loadstar Load Cell		Yes
P2-X(+) Load Cell	250 lb T+C Loadstar Load Cell		Yes
P3 Mooring Load Cell 3	250 lb T+C Loadstar Load Cell	Mooring Line	Yes
P3-Y Load Cell	250 lb T+C Loadstar Load Cell		Yes
P3-X(-) Load Cell	250 lb T+C Loadstar Load Cell		Yes
P3-X(+) Load Cell	250 lb T+C Loadstar Load Cell		Yes
P1 String Pot	12.5 in String Pot	Pod	Yes
P2 String Pot	12.5 in String Pot		Yes
P3 String Pot	12.5 in String Pot		Yes

Table 3 - Instrumentation on-board the scale model during basin testing

In the table above, P1 indicates a sensor positioned on Pod 1, P2 on Pod 2 etc. with Y, X+, and X-being the trio of load cells at the spar base. Additional string potentiometers were used for operational condition testing prior to the heave degree of freedom being locked for extreme condition testing.

In addition to the instrumentation listed in the table, LEDs were affixed to the backbone structure to allow for the natural point optical motion tracking system to record device kinematics.

Outside of these WEC-based instruments, the facility provided measurement systems for the water surface elevation in the form of wave probes placed along the bridge and below the carriage in the proximity of the WEC model. A complete list of the probes used can be found in the following table.

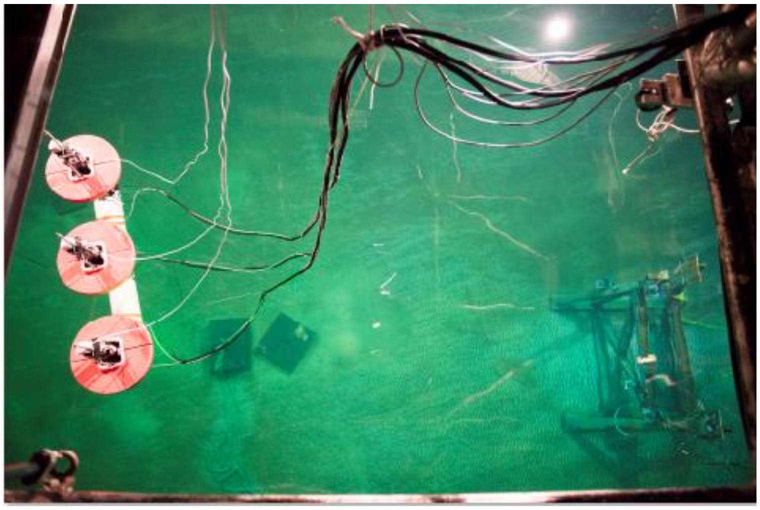

Figure 33 - Natural point tracking cameras were submerged in the basin (lower right of frame)

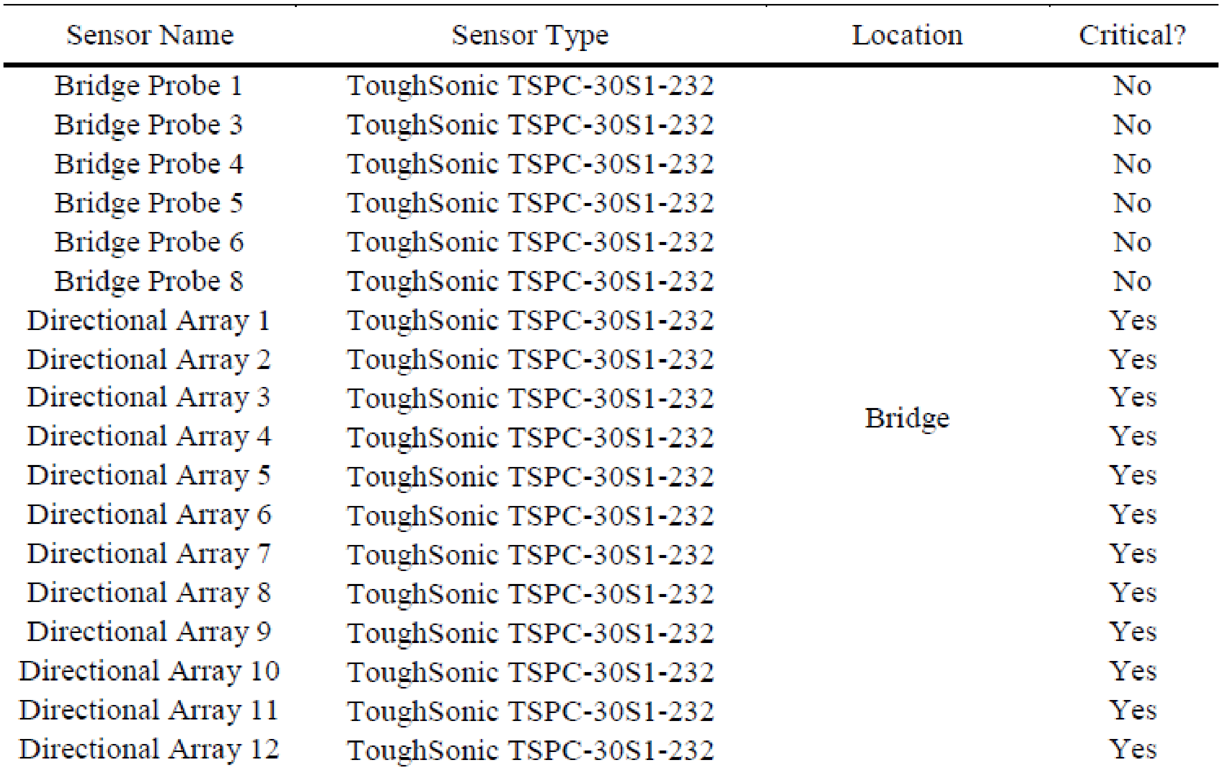

Sensor Name	Sensor Type	Location	Critical?
Bridge Probe 1	ToughSonic TSPC-30S1-232	Bridge	No
Bridge Probe 3	ToughSonic TSPC-30S1-232		No
Bridge Probe 4	ToughSonic TSPC-30S1-232		No
Bridge Probe 5	ToughSonic TSPC-30S1-232		No
Bridge Probe 6	ToughSonic TSPC-30S1-232		No
Bridge Probe 8	ToughSonic TSPC-30S1-232		No
Directional Array 1	ToughSonic TSPC-30S1-232		Yes
Directional Array 2	ToughSonic TSPC-30S1-232		Yes
Directional Array 3	ToughSonic TSPC-30S1-232		Yes
Directional Array 4	ToughSonic TSPC-30S1-232		Yes
Directional Array 5	ToughSonic TSPC-30S1-232		Yes
Directional Array 6	ToughSonic TSPC-30S1-232		Yes
Directional Array 7	ToughSonic TSPC-30S1-232		Yes
Directional Array 8	ToughSonic TSPC-30S1-232		Yes
Directional Array 9	ToughSonic TSPC-30S1-232		Yes
Directional Array 10	ToughSonic TSPC-30S1-232		Yes
Directional Array 11	ToughSonic TSPC-30S1-232		Yes
Directional Array 12	ToughSonic TSPC-30S1-232		Yes

Carriage 1	ToughSonic TSPC-30S1-232	Carriage	Yes
Carriage 2	ToughSonic TSPC-30S1-232		Yes
Carriage 3	ToughSonic TSPC-30S1-232		Yes
Carriage 4	ToughSonic TSPC-30S1-232		Yes
Carriage 5	ToughSonic TSPC-30S1-232		No
Wavemaker Pulse	EDL Hub TTL Pulse		Yes
Start Collect TTL	Function Generator		Yes
GPS Input	GPS Time Source	Wavemaker Room	Yes
Pod 1 Marker	NaturalPoint OptiTrack Marker	Centipod	Yes
Pod 2 Marker	NaturalPoint OptiTrack Marker	Centipod	Yes
Pod 3 Marker	NaturalPoint OptiTrack Marker	Centipod	Yes
Backbone Marker	NaturalPoint OptiTrack Marker	Centipod	Yes

Table 4 - Instrumentation provided by NSWCCD

The sea states tested were determined based on the contour method extreme sea states utilized in the numerical modelling. The largest individual wave for each of these sea states was run as a regular wave in repetition for at least 10 wave periods from broadside, and a 45-degree heading. Operational sea states were run as irregular waves for 200 times the wave period prior to extreme conditions. These operational sea states were selected based on the 6 sea states utilized by DOE's Wave Energy Prize [6] and two additional larger irregular sea states as a transition to the eventual extreme regular waves. The specifics of these sea states are shown in the table below.

Run Name	H_s, *MS ft*	T_p, *MS sec*	Direction, *deg*	Wave Type
O1	2.63	1.24	60	Irregular
O2	2.97	1.67	70	Irregular
O3	6.03	1.95	0	Irregular
O4	2.31	2.15	60	Irregular
O5	6.57	2.57	70	Irregular
O6	3.66	2.79	70	Irregular
O7	4.00	1.67	70	Irregular
O8	7.00	2.15	60	Regular
E1	21.586	2.03	70	Regular
E2	24.578	2.37	25, 70	Regular
E3	26.715	2.70	25, 70	Regular
E4	27.784	3.04	25, 70	Regular
E5	27.143	3.38	25, 70	Regular
E6	24.578	3.72	25, 70	Regular
E7	18.594	4.06	25, 70	Regular

Table 5 - Test cases run (MS- model scale)

In the table above, the wave direction is given relative to the MASK Basin bridge, which is angled at 70 degrees. Therefore, 70-degree waves are broadside to the WEC and 60 would be 10 degrees oblique. The tests were carried out roughly in the order outlined in the table with occasional re-runs for routine data acquisition errors and model mooring adjustments.

Figure 34 - Testing of model at MASK basin in baseline configuration.

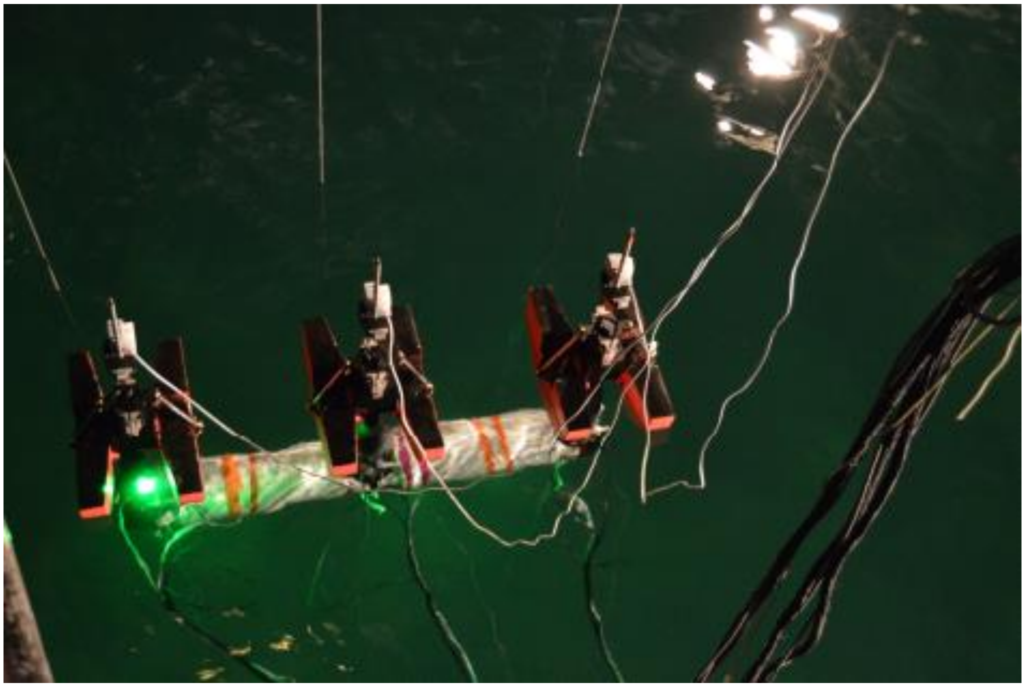

Figure 35 - Testing of model at MASK basin in folded configuration.

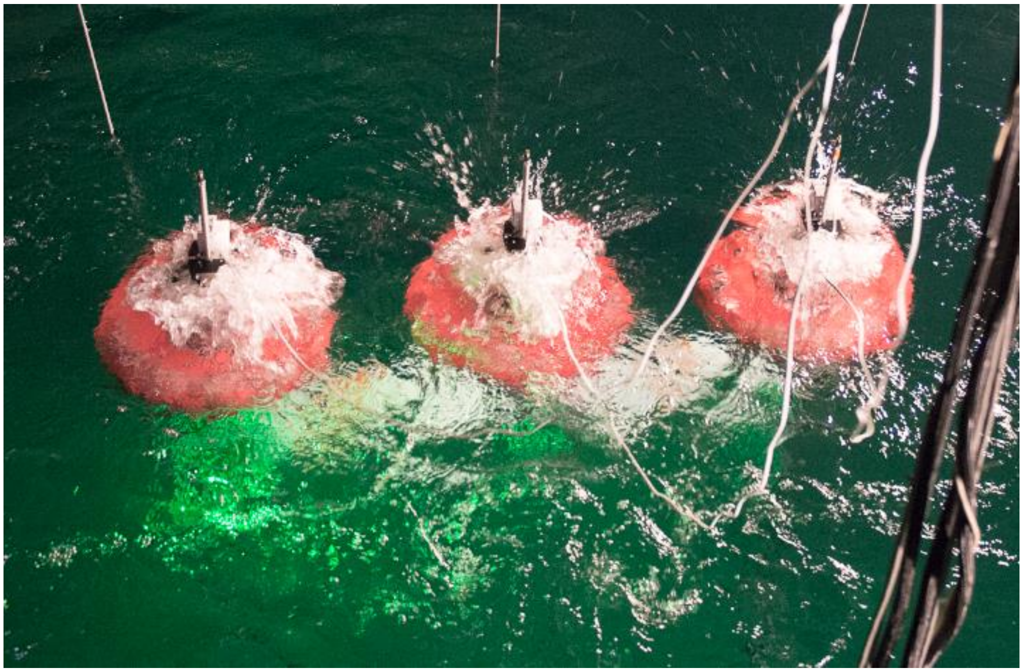

Figure 36 - Large wave crashing on model during test

Testing was successfully completed, gathering all desired data for this project. The following sections describe how the experimental data was used.

5.6 Task 6: Mid fidelity modeling of WEC

Building off the mid-fidelity WaveDyn model used for the down selection process, several improvements were made to the numerical model, including matching sea depth to the scale depth of the NSWCCD basin and improving the hydrodynamic representations of the bodies. Once testing data became available, actual model mass, moment inertia, and damping values were rolled into the model. Despite the progress made with WaveDyn, uncertainty over DNV-GL's desire to continue developing and supporting their WaveDyn software motivated Dehlsen Associates to evaluate their long-term design tool choices.

Consequently, in the months after the wave basin testing, a parallel model was set-up in WEC-Sim, an open-source code for simulating wave energy converters developed in MATLAB/Simulink using the multi-body dynamics solver Simscape Multibody [8]. This was an additional mid-fidelity model that was not initially planned in the scope, but circumstances allowed for the creation of this model with minimal investment. The national labs team at NREL and Sandia needed to build a model of the WEC for their high-fidelity work scope, which allowed the team to readily assist in the creation of a mid-fidelity Centipod model in WEC-Sim. WaveDyn and WEC-Sim yielded similar results when directly compared, giving confidence to the usage of either model. The WEC-Sim model fit seamlessly into the workflow for the overall project team, being easily customized and run in the MATLAB environment, which was already being used for experimental data post processing. On the balance of all technical and programmatic considerations, the WEC-Sim model was selected for validation in this project over the WaveDyn model.

The WEC-Sim model was compared against the experimental data to validate the numerical model. This work was conducted by NREL and a summary of the results at model scale is presented in the following figures.

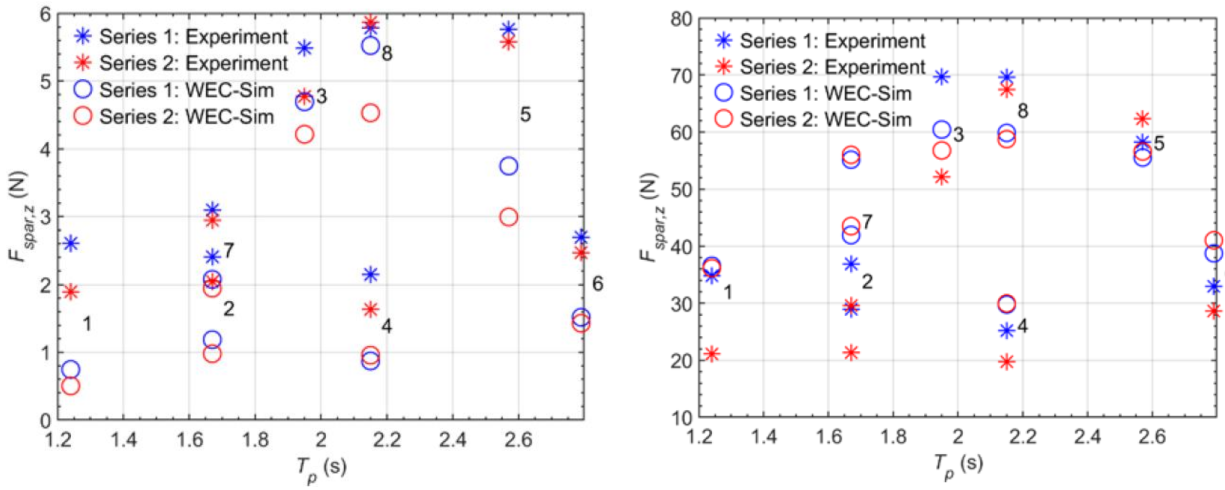

Figure 37 – Force Spar, z: median loads for fatigue (left), ultimate loads (right)

Force Spar *z* or commonly referred to in this report as Spar axial force, is shown in Figure 37 with both the equivalent fatigue loads over the sea state and the ultimate loads presented. The sea states labeled as 1-8 are listed as O1-O8 in Table 5 for reference. Alignment between the numerical model and experimental data was generally very good for this load assessment.

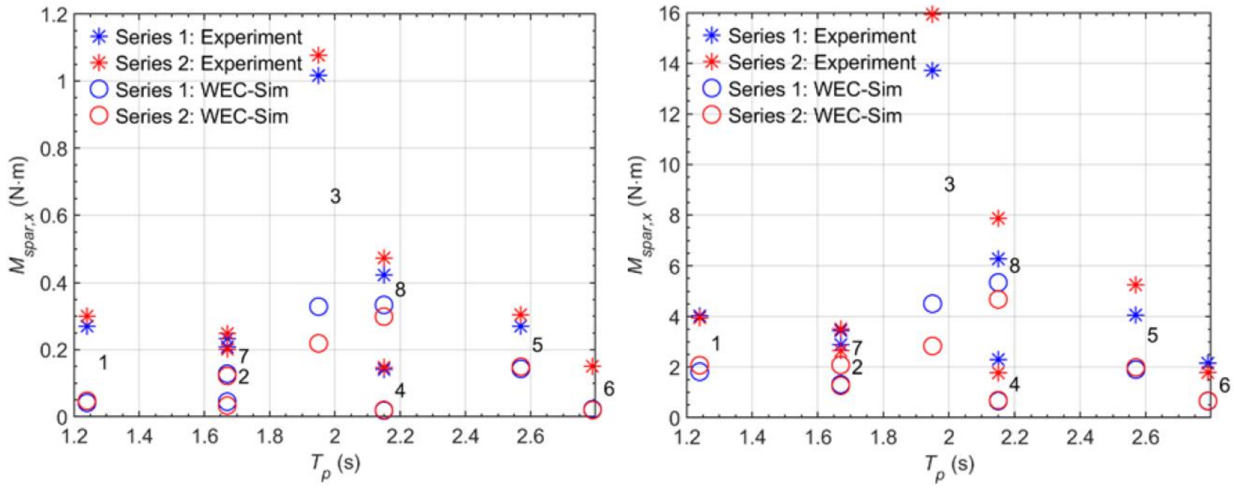

Figure 38 – Moment Spar, x: median loads for fatigue (left), ultimate loads (right)

Moment Spar *x* is the pitch rotational axis moment imparted on the Spar at the base where it connects to the Backbone. This moment is expected to be the larger of the two spar moments measured due to the WEC orientation with the wave heading. The numerical model struggles with the 70-degree wave heading in sea state 3, but otherwise gives a fairly reliable prediction of pitch moments.

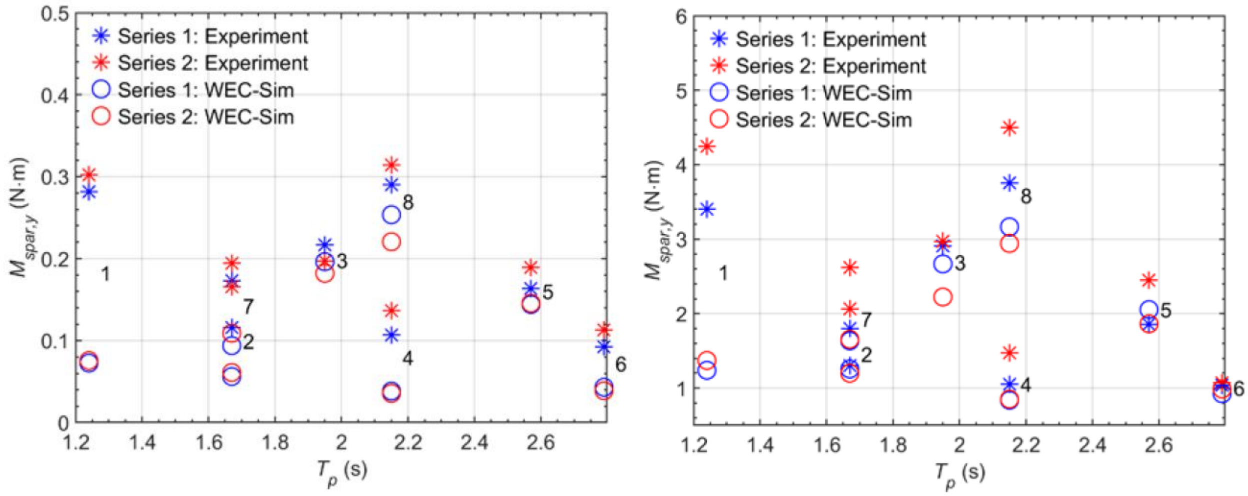

Figure 39 - Spar y: median loads for fatigue (left), ultimate loads (right)

Moment Spar, *y*, is the roll rotational axis moment imparted on the Spar at the base where it connects to the Backbone. Numerical model results once again are consistent with experimental data.

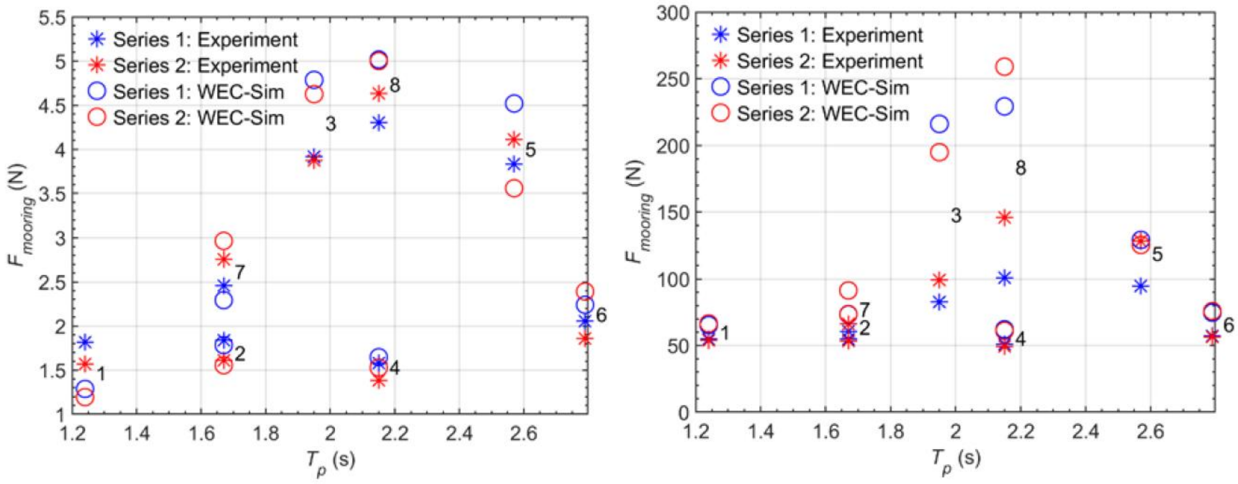

Figure 40 - Mooring Tension: median loads for fatigue (left), ultimate loads (right)

Finally, mooring line tension is shown in Figure 40. Results are good across the board with the exception of very conservative load prediction in the large sea state, 8 and the 70-degree sea state, number 3.

The conclusions from the validation study as written by the NREL team were as follows:

"*The differences between the experimental and WEC-Sim derived power and loads are well within the expected limitations of linear-based modeling and experimental error. Given these results, the Centipod WEC-Sim model has been validated, and could foreseeably be used, along with standard* *safety factors, to design and simulate the Centipod's power production, operational design loads, and fatigue life."*

With respect to the WEC-Sim derived power production of the WEC in comparison to experimental testing in the wave basin, the results were also favorable.

"*The average difference between the experimentally derived Pavg and WEC-Sim derived Pavg is 30.14%. The average difference between experimentally derived Pavg for Test Series 1 and 2 is 15.72%, which gives an indication of the experimental error/repeatability. The more nonlinear wave conditions (corresponding to higher Hs) have higher error, while the more linear wave conditions have lower error, which may be expected for the linear-based WEC-Sim model.*"

5.7 Task 7: High fidelity modeling of WEC

High fidelity modeling was completed by NREL and set-up of the Computational Fluid Dynamics (CFD) models is explained in great detail within the *International Conference on Offshore Mechanics and Arctic Engineering* paper written as the result of this work [9].

STAR-CCM+ [10] was used in this high-fidelity CFD simulation study. The large, complicated structure inherent to Centipod's multi point absorber topology made CFD simulations computationally expensive and time consuming. As a result, the largest individual wave within the largest sea state was the case for examination though high-fidelity methods in this project. This case was simulated for both the operational and survival WEC configurations with both a broadside (0-degree) and 45-degree wave heading for a total of four extreme load CFD simulations. The Pods were locked in the heave degree of freedom as they were for the wave basin testing to maintain consistency and simplify the simulation.

The mooring lines were modeled with simple linear spring couplings with no repelling force such that snap and slack mooring loads ($F_{mooring}$) are simulated. To model the structural loads (F_{PTO} and M_{spar}), a one-way FEA coupling approach was used. At each timestep, the pressure, shear, and mooring forces were mapped to a separate STAR-CCM+ FEA simulation of the Centipod. The one-way FEA coupling approach is acceptable for these simulations because the structural components are nearly rigid, and any response of the structure on the fluid dynamics is negligible.

The STAR-CCM+ computational domain and grid refinement zones are presented in Figure 41 below. Regular waves were modeled for the scale Centipod model using the MASK Basin depth and a width twice the depth, which is approximately 10 times the Centipod WEC width. The computational domain length was adjusted such that there was ~2λ in front of, and ~4λ behind, the WEC model. A velocity inlet with a fifth-order regular wave were specified at the channel inlet and side walls. A pressure outlet, with 2λ wave damping to minimize wave reflections, was specified at the channel outlet. Slip walls were specified at the top and bottom walls. The grid shown in Figure 41 was obtained via mesh resolution and convergence studies. The grid refinement zones were based on minimizing the average y+ on the WEC model surface, as well as sufficiently resolving the velocity gradients surrounding the model, while keeping the total number of cells at a minimum. The resulting grid resolution at the water surface was $\lambda/\Delta x$=138 in the horizontal direction, H/Δz=40 in the vertical direction, and an average $y+$ of 19.2 on the model surface. The average number of cells used for each of the validation simulations is 18.8x10^6. Each of the simulations is run for 20T using second-order temporal accuracy, and time steps corresponding to a Courant number ($C = u\Delta t/\Delta x_{\min}$) of 0.5 to ensure numerical stability and accuracy.

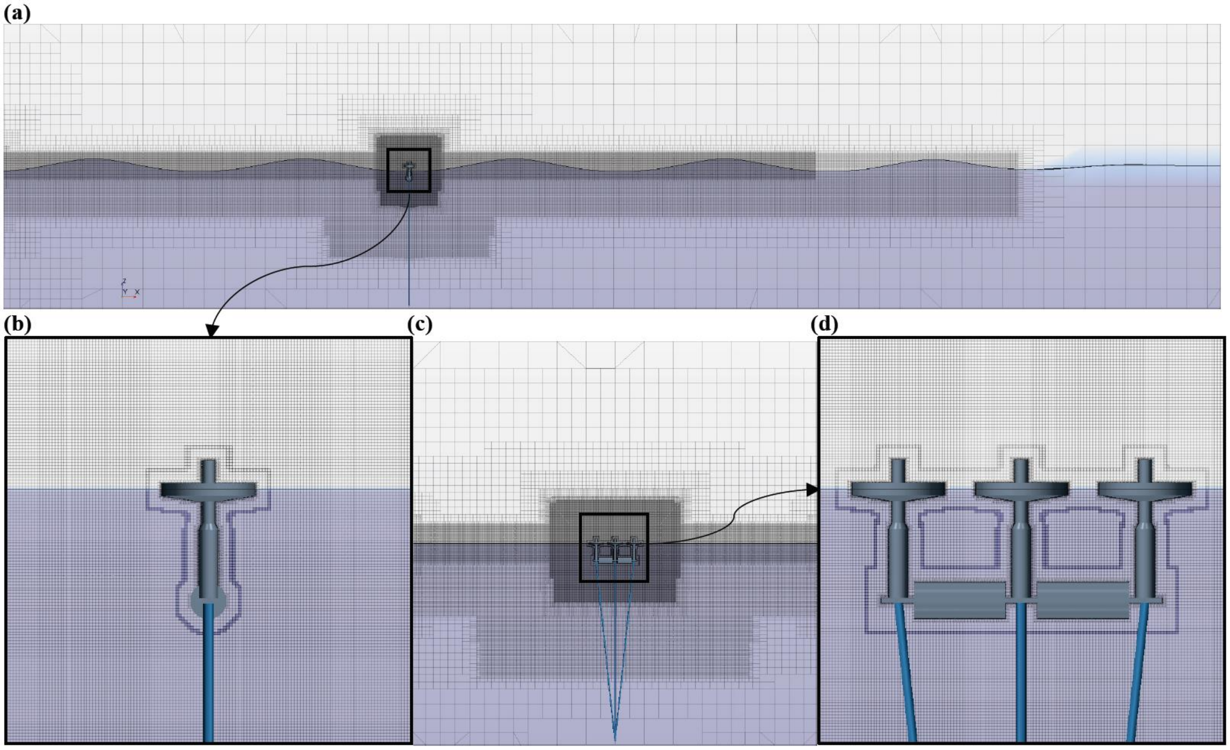

Figure 41 - STAR-CCM+ computational domain and grid refinement zones for the operational Centipod configuration: (a) Side view, (b) side view detail, (c) front view, (d) front view detail

Each simulation required 17 days and used 672 CPU cores on average, for a total of ~2.8x10^5 CPU-hours. The resulting ratio of simulation time to real time was ~2.1x10^4.

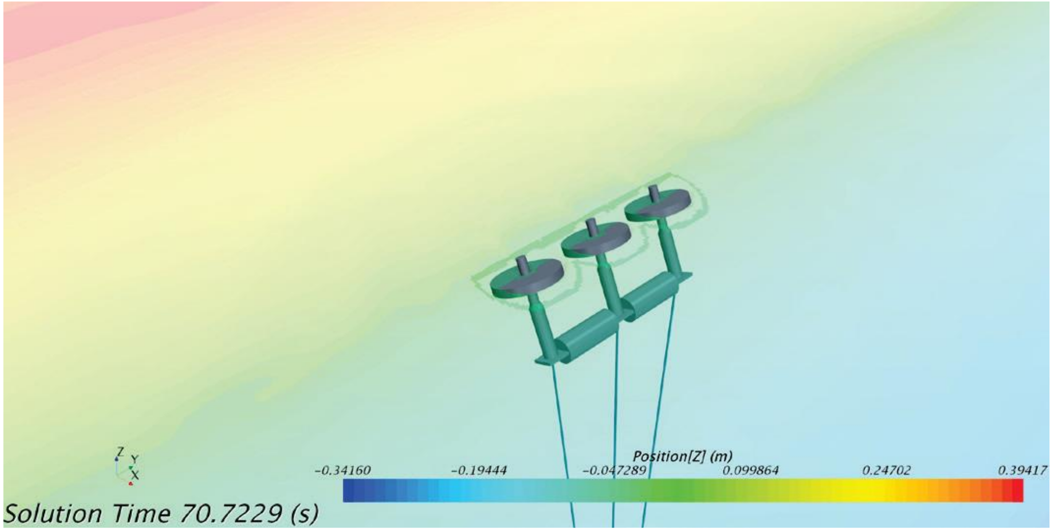

Figure 42 - STAR-CCM+ Extreme wave simulation 5, for baseline configuration with 0deg wave heading.

High fidelity STAR-CCM+ simulations were compared to experimental data from the wave tank testing. A selection of results is shown in the figures below at model scale.

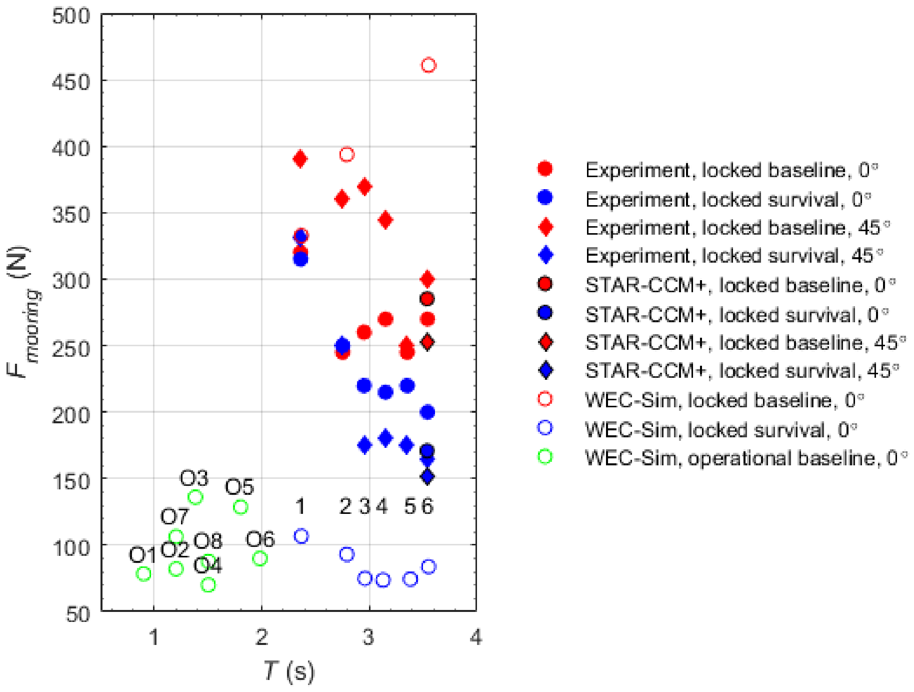

Figure 43 - Mooring line Tension ($F_{mooring}$). Experimental data, vs High-fidelity, vs WEC-Sim

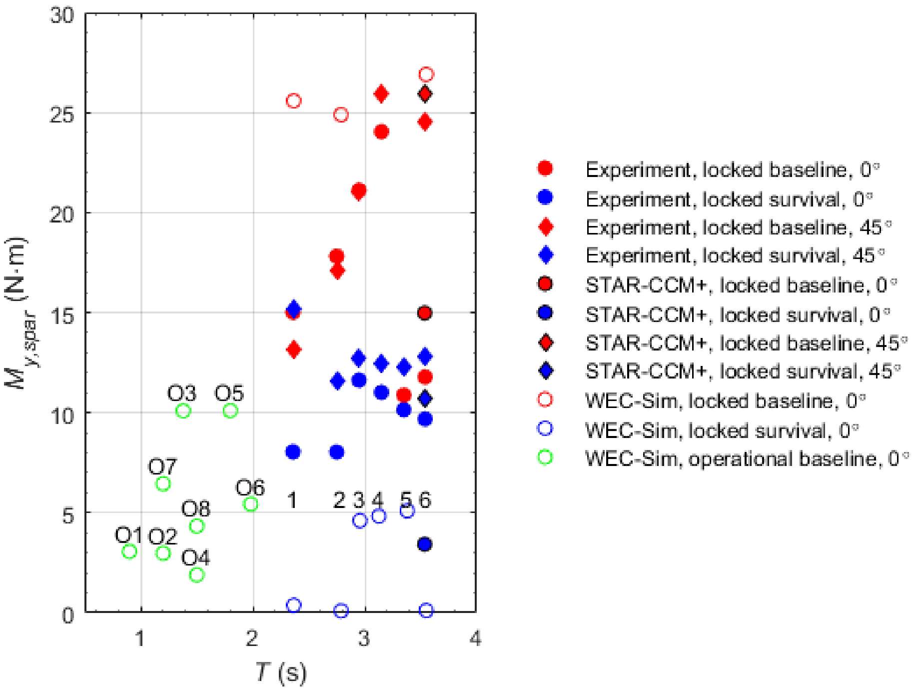

Figure 44 - Pod-Spar Moment (M_{spar}). Experimental data, vs High-fidelity, vs WEC-Sim

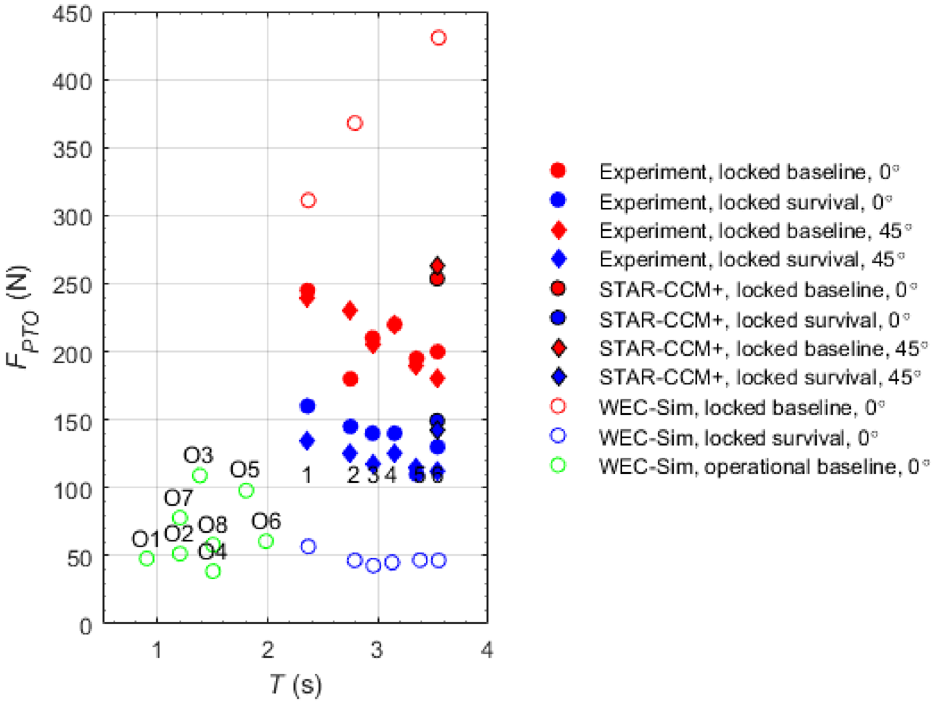

Figure 45 - Pod-Spar Axial Force (F_{PTO}). Experimental data, vs High-fidelity, vs WEC-Sim

The STAR-CCM+ results are relatively good compared to the experimental data across the board. Based on the F_{PTO} and $F_{mooring}$ results, it appears that WEC-Sim significantly overpredicts these loads in the baseline configuration and slightly under predicts F_{PTO} and $F_{mooring}$ in the survival configuration. However, both WEC-Sim and STAR-CCM+ results indicate a significant load reduction in F_{PTO}, $F_{mooring}$, and M_{spar} for the survival configuration.

5.8 Task 8: Impact Analysis

The impact of this project is largely broken down into two areas for assessment: the evaluation of design tools for usage in the development process with respect to extreme loads, and the impact of the chosen load mitigation strategy on the viability of the Centipod WEC from an LCOE standpoint. The latter also more generally covers all proposed project metrics leading to the LCOE.

5.8.1 Design Tool Evaluation

The mid-fidelity WEC-Sim model is a capable tool for prediction of loads under operational conditions as shown in Section 5.6. While the validation of this model for the Centipod WEC was a significant milestone for this project and development process, the outcome itself was not particularly surprising. The wave energy sector has come to expect reliable results from WEC-Sim and other mid-fidelity tools for operational sea states so long as they are used correctly and the WEC parameters fed into the model are realistic. The challenge was then whether a mid-fidelity tool could be used for exploration of design concepts for the purposes of extreme load evaluation. Extreme loads are, as clearly demonstrated throughout this project, often an order of magnitude larger than operational loads. This presents different problems than when used for simulations in small and moderate waves, with the most obvious limitation being the linear theory basis of the model confronting non-linear hydrodynamic conditions. That weakness is concurrently a strength as the linear basis allows these codes to run simulations in minutes or hours, making them very useful when the output is credible. Meanwhile, the high-fidelity model is well equipped for the challenge and should theoretically do an excellent job given enough time and computational power, often several weeks per simulation.

As concluded in the associated paper on the creation of both models for this project [9], prior to the eventual WEC-Sim model improvements and turning the STAR-CCM+ versus WEC-Sim (high-fidelity vs mid-fidelity) comparison of the heave response for the baseline configuration was an encouraging indication of WEC-Sim's capabilities to simulate a WEC's first-order response in extreme sea states. These results indicated that WEC-Sim models can provide reasonable design results at a fraction of the computational expense of CFD/FEA. However, the STAR-CCM+ versus WEC-Sim comparison of the heave response for the survival configuration was indicative of the challenges of linear-based models. Generally, linear-based models, particularly in extreme sea states, require significant tuning to CFD and experimental data, which may not always be available.

The WEC-Sim model developed in this project can theoretically be improved by including nonlinear Froude-Krylov forcing terms, but in practice this resulted in much longer simulation times while only yielding a marginal improvement. The WEC-Sim model was however improved by tuning the viscous drag coefficients based on experimental data, an advantage that is only available if experimental testing has been completed as it had in this case. Furthermore, WEC-Sim itself was improved to account for large transient yaw motions as the result of this observed shortcoming during this project.

WEC-Sim significantly overpredicts F_{PTO} and $F_{mooring}$ loads in the baseline configuration and slightly under predicts F_{PTO} and $F_{mooring}$ in the survival configuration. However, both WEC-Sim and STAR-CCM+ results indicate a significant load reduction in F_{PTO}, $F_{mooring}$, and M_{spar} for the survival configuration. The 45-degree wave heading had minimal impact on F_{PTO} and $F_{mooring}$ in the STAR-CCM+ simulations, but M_{spar} was increased with this heading in the baseline configuration, while decreased in the survival configuration. Given that the 45-degree wave heading affects the rotational degrees of freedom more significantly than the translational degrees of freedom, these results appear to be reasonable.

In summary, mid-fidelity tools such as WEC-Sim are a valuable part of the extreme condition design process and can provide useful information as to the relative loads of different parameters. The accuracy of the results is improved with the availability of experimental data for model tuning, but even after tuning engineers should remain vigilant of the shortcoming of linear models, and take the ultimate loads obtained from mid-fidelity tools as indicative until proven by high-fidelity simulations or experimental testing.

5.8.2 Project Metric Attainment

Three main metrics were proposed within this project. These were axial force in the spar, installed capital cost (ICC), and Levelized Cost of Energy (LCOE). All three are important, but LCOE is the ultimate metric for emerging renewable technologies striving for economic viability, as LCOE improvement is the goal. ICC is merely a component of the LCOE, and the axial force is further a component of ICC.

The methodology used for LCOE analysis in this project follows DOE LCOE reporting guidance [11] wherever possible. LCOE is calculated with an FCR of 0.108 and the standardized formula of:

$$LCOE = \frac{ICC * FCR + O\&M}{AEP} \qquad (1)$$

Where:

ICC – Installed Capital Cost ($)
FCR – Fixed Charge Rate
O&M – Operations & Maintenance ($/yr)
AEP – Annual Energy Production (MWh/yr)

To explain the project metrics most effectively, they should be discussed in order of their cascading effects starting with maximum load reduction.

Metric	Proposed Improvement	Achieved Improvement
Maximum Pod Axial Force (kN)	42%	27%
ICC ($/kW)	8%	10%
LCOE ($/kW-h)	6%	8%

Table 6 - Project metrics proposed and attained

Maximum Pod Axial Force

Beginning with the foundation of the cascading trio of project metrics, maximum force reduction is at the core of the proving the project hypothesis. It is not a given that a load mitigation strategy will certainly reduce loads in extreme conditions until it is thoroughly modelled and tested. That caution aside, in this project the results of the folded survival strategy were, as implied throughout this report, very favorable.

When comparing the largest loads of any sea testing in baseline to the largest loads of any sea tested in the folded configuration, we see a 27% reduction in maximum load. It is worth noting that in most sea states tested, the load reduction from baseline to folded under the same conditions was even more significant. The 45-degree wave heading in the shorter steeper Extreme Sea State 1 proved challenging enough for the survival method to yield a narrower margin due to that condition. In the larger longer period waves the folded configuration opens up a wider advantage.

axial F	baseline	folded	% of base	% reduction
MS Force (N)	241	175	73%	27%

Table 7 - Axial Force load reduction results

Of most interest is of course the relative change in loads between baseline and folded. While this 27% reduction falls short of the proposed 42% reduction it is not the whole story of loads reduction. The mooring load reduction achieves a similar load reduction to the axial force, but the pitch degree of freedom spar moment makes a strong case for the folded configuration

pitch M	baseline	folded	% of base	% reduction
MS Moment (Nm)	28	16	57%	43%

Table 8 - Spar Moment reduction reults

A large 43% reduction in maximum moment is achieved by the folded configuration, which happens to meet the aspiration for load reduction in axial force. Both loads are applied to the same structure, and both axial loading and toque in the structure due to the moment affect the design objective for wall thickness in the spar. The combined effects of these loads into the design of the WEC and impact the machine’s capital cost.

Installed Capital Cost (ICC)

Taking the effects of load reduction and rolling them into ICC reduction required structural analysis and costing studies. To approach this evaluation, the cost model for Centipod was stripped down to the lowest common capital cost between the two variants, i.e. the cost of the base machine with one degree of freedom and the lowest load conditions. From this point, the costs of each option were layered on. In the case of the baseline, the costs associated with higher loads were added, for the folded case, the additional degree of freedom mechanism was added to the common capital cost base.

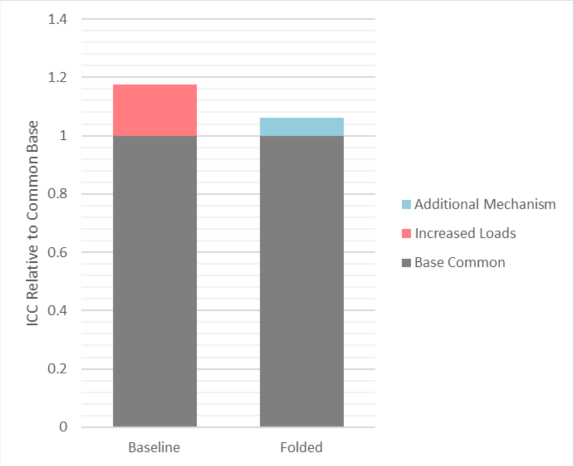

Figure 46 - Relative ICC comparison

In both cases the structure was studied to find the change in mass of components as the result of wall thickness or geometry changes required to handle the designed loads. In some cases, the structural impact could be covered analytically with simple equations, while in other cases, Fine Element Analysis (FEA) was used to determine the structural mass of components. In many cases this was an iterative process with components being designed, run through FEA, then refined to reduce localized stresses. One step within the iterative design process of a linkage in the folding mechanism is shown as example in Figure

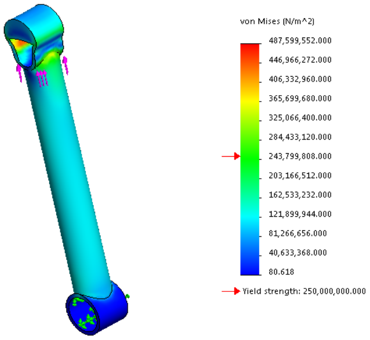

Figure 47 – Linkage in FEA

47. The resulting component masses were used in conjunction with a given cost per mass of steel to determine capital cost impacts.

As seen in Figures 46, the folded configuration is a clear winner when evaluated in terms of installed capital cost. This difference can be more clearly seen as we break down the major cost associated with each configuration.

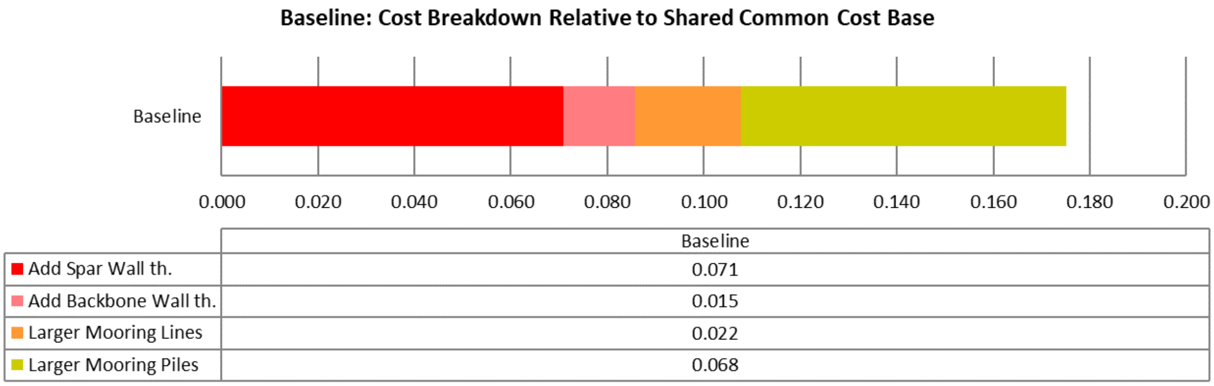

	Baseline
■ Add Spar Wall th.	0.071
■ Add Backbone Wall th.	0.015
■ Larger Mooring Lines	0.022
■ Larger Mooring Piles	0.068

Figure 48 - Baseline additional cost breakdown

And plotted as relative cost again referencing the lowest common capital cost on the same 0-20% axis for both figures, the Folded configuration:

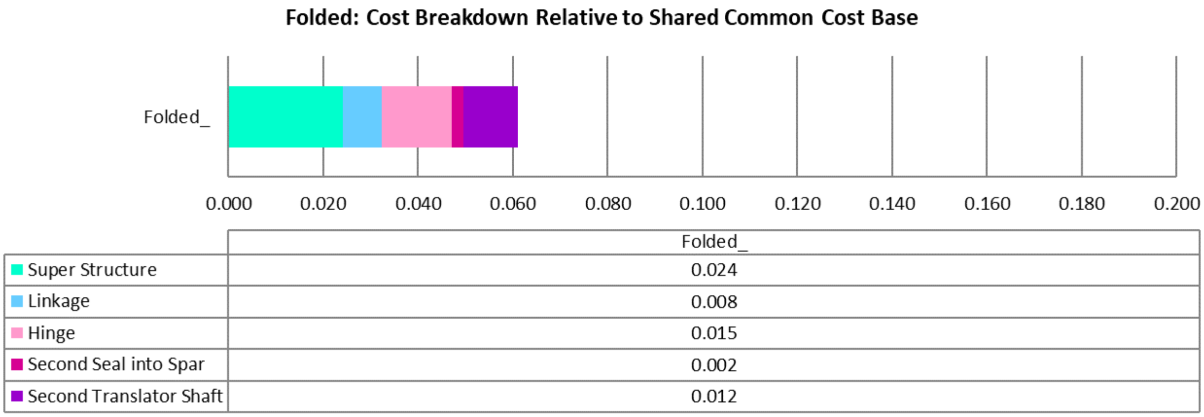

	Folded_
■ Super Structure	0.024
■ Linkage	0.008
■ Hinge	0.015
■ Second Seal into Spar	0.002
■ Second Translator Shaft	0.012

Figure 49 - Folded additional cost breakdown

The folded configuration represents a 10% reduction in capital cost over the baseline case. This is due to larger costs of the structure itself, and more significantly increased costs in the mooring components. This cost reduction outperforms the proposed 8% cost reduction metric by a large margin due primarily to more focus being put on the WEC structural costs than mooring costs when designing the project metrics. This ICC reduction sets the stage for a promising LCOE impact result.

Levelized Cost of Energy (LCOE)

Finally, the previous metrics build into the ultimate test of viability for a new design configuration, LCOE. If we return to the basic LCOE formula (1) from the beginning of this section, the pieces start to come together:

ICC: 10% reduction

FCR: No Change

O&M: Negligible Change

AEP: No Change

LCOE: 8% reduction

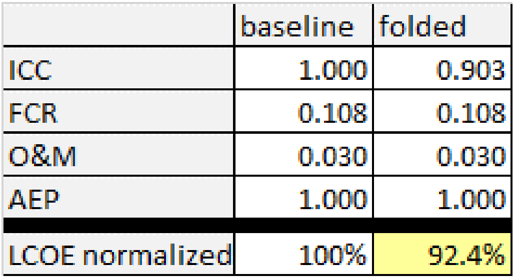

	baseline	folded
ICC	1.000	0.903
FCR	0.108	0.108
O&M	0.030	0.030
AEP	1.000	1.000
LCOE normalized	100%	92.4%

Figure 50 - Normalized LCOE

Beyond the ICC and the other factors that are unchanged by the load mitigation configuration selection. FCR, obviously is fixed the LCOE reporting guidance [11]. Even if it were not fixed artificially, the components of FCR are generally unchanged by the folded configuration barring the arguable, but weak, premise that perhaps reduced extreme condition risk would lead to a more favorable cost of capital. AEP is unchanged; the device hydrodynamics are unchanged for the operational mode and power extraction would therefore be identical, setting aside an interesting note for future exploration that will be made in the conclusion of this report for the time being. O&M is then the only possible variable to change.

O&M is notoriously challenging to predict at this stage of development (TRL 4), and this report does not conclude that it would play a major factor in the LCOE impact of a folded configuration. The considerations to be discussed are:

Marine Operations Cost: The load reduction in the folded configuration results in smaller piles and smaller diameter mooring lines. It is conceivable that the size reduction of these components could affect the vessel chosen for marine operations (ether install or ongoing maintenance). However, in the installation investigation conducted in this project with InterMoor where real vessel sizes were considered, the piles were not near on the cusp of vessel selection. Vessel selection as a result of maximum loads remains a consideration as the WEC is carried forward in its development path, but it was left as a negligible impact in this study.

Additional Failure Modes: Adding another degree of freedom means there are more moving parts in the machine and therefore more failure modes (e.g. seal failures, bearing failures, etc.). This was considered, but relative to the overall WEC installed capital cost, the new mechanism represents just over 6% of the total device ICC. At 6% of ICC replacement, replacement parts aren't likely to drive the O&M significantly. Moreover, the counterargument is the overall reduced ICC of the device in the folded configuration could actually be seen to reduce O&M costs as at TRL 4 treating O&M as a fixed percentage of ICC is not an uncommon approach.

Because of the confidence in O&M costs associated with the change and the existence of rational arguments for both a lower and higher O&M, maintaining the same absolute O&M for both cases was concluded to be the conservative assumption for the sake of this trade study.

With O&M maintained across the two variants, LCOE could be run for both cases as seen in a set of normalized results in Figure 50. The result of the folded load mitigation strategy, LCOE is reduced by 8%, exceeding the proposed LCOE improvement metric for this project.

6.0 Accomplishments

This project proved the merit of an additional degree of freedom being added to a WEC for the purposes of load mitigation and survival strategy. Of particular note was the resulting LCOE endorsement of the folding survival configuration when a trade study was conducted using a combination of direct experimental model scale data and numerical model simulations. The LCOE improvement resulting from this project greatly exceeded expectations and confirms the design path taken is a valuable area of study for the Centipod WEC and other wave energy converters in general.

With regard to furthering the development of the Centipod wave energy converter, this project advanced the technology into TRL 4, seeing wave basin testing of the operational and survival configurations and validating the numerical tools used for design and simulation for not just energy production purposes but load prediction as well.

Throughout the project, an overarching question of which tools were suitable for exploring the survival design space was under evaluation. This project concluded that, in addition to computational fluid dynamics (high-fidelity models) and experimental testing at scale, mid-fidelity tools such as WEC-Sim deserve a place in the design workflow with respect to extreme loads. While limitations exist for such numerical tools, these simulations consistently provided a clear understanding of the relative loads when evaluating two design configurations, suitably steering the design path in a focused direction where more refined tools could be employed. This should be a beneficial take-away for the wider sector as design workflows are established for a variety of MHK technologies.

Finally, this project yielded an opportunity to improve the open source WEC-Sim code for sector-wide benefit, as the ability to better simulate transient yaw motions [9], [12] in WECs was added to the code following the validation work conducted by the national laboratories.

7.0 Conclusions

Extreme loads act as structural design drivers and one of the principal causes of the current economic viability gap for wave energy converters. Reducing extreme loads by even a small margin produces an impactful LCOE result. However, paying for load reduction in the form of increased capital expense for a load mitigation strategy can be a difficult concept to evaluate without a clear understanding of the strategy's loads impact. This project achieved a good understanding of loads with and without a mitigation strategy in place though the employment of mid-fidelity models, high-fidelity models, and scaled wave basin testing. Furthermore, this project presented a strong argument that the additional capital expense enabling a load mitigation strategy is worthwhile in this case, and presumably many others.

The LCOE reduction resulting from this work exceeded the project expectation and will serve to increase confidence in the design tools, loads, and choices as the Centipod WEC is brought closer to technical maturity. Moreover, the viability of an additional degree of freedom for the transition into the folded survival configuration grants motivation for future work to explore usage of this mechanism enabling WEC enhancements in installation, operation, and power capture to further capitalize on LCOE reduction.

8.0 References

[1] “Power from sea waves,” *Adv. Water Resour.*, vol. 4, no. 2, p. 97, Jun. 1981, doi: 10.1016/0309-1708(81)90034-8.

[2] D. S. Jenne, Y.-H. Yu, and V. Neary, “Levelized Cost of Energy Analysis of Marine and Hydrokinetic Reference Models: Preprint,” 2015. Accessed: Oct. 06, 2020. [Online]. Available: www.nrel.gov/publications.

[3] F. Kreith and D. W. Pepper, “Energy Efficiency and Renewable Energy - Next Generation Marine Energy Systems - Durability and Survivability,” 2014.

[4] A. R. Dallman and V. S. Neary, “Characterization of U.S. Wave Energy Converter (WEC) Test Sites: A Catalogue of Met-Ocean Data,” 2014. Accessed: Sep. 18, 2020. [Online]. Available: http://www.ntis.gov/help/ordermethods.asp?loc=7-4-0#online.

[5] “WDRT : A Toolbox for design-response analysis of wave energy converters.” https://www.researchgate.net/publication/308794966_WDRT_A_Toolbox_for_design-response_analysis_of_wave_energy_converters (accessed Sep. 18, 2020).

[6] D. Bull and A. Dallman, “Wave energy prize experimental sea state selection,” in *Proceedings of the International Conference on Offshore Mechanics and Arctic Engineering - OMAE*, Sep. 2017, vol. 10, doi: 10.1115/OMAE2017-62675.

[7] P. A. Brodtkorb, P. Johannesson, G. Lindgren, I. Rychlik, J. Rydén, and E. Sjö, “WAFO - A Matlab Toolbox For Analysis of Random Waves And Loads,” Jan. 2000.

[8] Y.H. Yu, M. Lawson, K. Ruehl, and C. Michelen, “DEVELOPMENT AND DEMONSTRATION OF THE WEC-SIM WAVE ENERGY CONVERTER SIMULATION TOOL,” 2014.

[9] J. Van Rij, Y.-H. Yu, A. McCall, and R. G. Coe, “Extreme load computational fluid dynamics analysis and verification for a multibody wave energy converter,” in *Proceedings of the International Conference on Offshore Mechanics and Arctic Engineering - OMAE*, 2019, vol. 10, doi: 10.1115/omae2019-96397.

[10] “STAR-CCM+.” https://www.plm.automation.siemens.com/global/en/products/simcenter/STAR-CCM.html (accessed Sep. 29, 2020).

[11] A. LaBonte, P. O. Connor, C. Fitzpatrick, K. Hallett, and Y. Li, “Standardized Cost and Performance Reporting for Marine and Hydrokinetic Technologies,” *1st Mar. Energy Technol. Symp.*, no. March, pp. 1–10, 2013.

[12] “Release WEC-Sim v4.1 · WEC-Sim/WEC-Sim · GitHub.” https://github.com/WEC-Sim/WEC-Sim/releases/tag/v4.1 (accessed Oct. 06, 2020).